




## Article

# Multilayer Sheets Based on Double Coatings of Poly(3-hydroxybutyrate-co-3-hydroxyvalerate) on Paper Substrate for Sustainable Food Packaging Applications

Eva Hernández-García <sup>1</sup>, Pedro A. V. Freitas <sup>1</sup>, Pedro Zomeño <sup>2</sup>, Chelo González-Martínez <sup>1</sup>  
and Sergio Torres-Giner <sup>1,\*</sup>

<sup>1</sup> Research Institute of Food Engineering for Development (IIAD), Universitat Politècnica de València (UPV), 46022 Valencia, Spain

<sup>2</sup> Packaging Technologies Department, AINIA, 46980 Paterna, Spain

\* Correspondence: storresginer@upv.es

**Featured Application:** One of the main technological challenges within Circular Economy strategies is to minimize the environmental impact of plastic packaging. In this regard, the use of PHBV films to coat paper sheets represents a highly sustainable strategy to produce food packaging multilayer structures with improved mechanical and barrier properties.

**Abstract:** This work reports on the development and performance evaluation of newly developed paper sheets coated, on both sides, with thin films of biodegradable poly(3-hydroxybutyrate-co-3-hydroxyvalerate) (PHBV) for applications of food packaging. For this, PHBV/paper/PHBV multilayers were first prepared by the thermo-sealing technique, optimizing the process variables of temperature and time. Thereafter, the multilayer sheets were characterized in terms of their morphological, optical, thermal, mechanical, and barrier properties and compared with equivalent paper structures double coated with high-barrier multilayer films of petrochemical polymers. The results indicated that the double coatings of PHBV successfully improved the mechanical resistance and ductility, protected from moisture, and also reduced the aroma and oxygen permeances of paper, having a minimal effect on its optical and thermal properties. Finally, the compostability of the resultant multilayer sheets was analyzed, confirming that the presence of the PHBV coatings slightly delayed the aerobic biodegradation and disintegration of paper.

**Keywords:** paper; PHBV; multilayers; food packaging; Circular Economy



**Citation:** Hernández-García, E.; Freitas, P.A.V.; Zomeño, P.; González-Martínez, C.; Torres-Giner, S. Multilayer Sheets Based on Double Coatings of Poly(3-hydroxybutyrate-co-3-hydroxyvalerate) on Paper Substrate for Sustainable Food Packaging Applications. *Appl. Sci.* **2023**, *13*, 179. <https://doi.org/10.3390/app13010179>

Academic Editor: Hyeonseok Yoon

Received: 7 December 2022

Revised: 19 December 2022

Accepted: 20 December 2022

Published: 23 December 2022



**Copyright:** © 2022 by the authors. Licensee MDPI, Basel, Switzerland. This article is an open access article distributed under the terms and conditions of the Creative Commons Attribution (CC BY) license (<https://creativecommons.org/licenses/by/4.0/>).

## 1. Introduction

Packaging increases food quality and safety, which is essential to avoid spoilage and reduce food waste [1]. Plastic represents, together with paper, the most widely used material for food packaging applications due to its large-scale availability, low production cost, light weight, transparency, flexibility, good barrier, ease of processing, and versatility [2]. However, despite these advantages, conventional plastics are still based on petrochemical polymers that are synthesized from a non-renewable source and are not biodegradable. Moreover, these plastics are difficult to recycle, particularly when they are found in the form of multilayers. As a result, plastic packaging represents a major source of waste generation and plastics easily accumulate in the environment [3]. In fact, plastic materials can take between 100 and 450 years to disintegrate in the environment, leading to the so-called “white pollution” and to the formation of marine debris and microplastics [4]. In addition, microplastics can be taken up by different species in the food chain, which is a growing concern for human health and natural habitats [5].

Therefore, one of the main current challenges is to minimize the environmental impact of plastic packaging. From this perspective, the use of paper in packaging recently repre-

sents a sustainable option due to its biodegradable nature and the fact that it can be more easily recycled than plastic. However, paper lacks moisture resistance and shows poor thermal, mechanical, and barrier performances so that it is habitually coated with plastic materials [6]. Thus, multilayer packaging structures based on paper have expanded tremendously during the past few years, with use of different coating technologies to offer several functionalities, such as hydrophobicity, a gas and moisture barrier, antimicrobial protection, cohesive strength, scratch resistance, etc. [7]. Different petrochemical polymers have been used for coating paper, including polypropylene (PP) and biaxially oriented polypropylene (BOPP), low- and high-density polyethylene (LDPE, HDPE), polyethylene terephthalate (PET), biaxially oriented polyamide (OPA), and more importantly their combinations in the form of multilayers with high-barrier poly(ethylene-co-vinyl alcohol) (EVOH) [8]. These plastic multilayers have been demonstrated to increase the barrier against moisture, oxygen, odor, and grease, and offer favorable stiffness, toughness, processability, manufacturing cost, chemical resistance, and thermal stability. Nevertheless, these are not biodegradable and must be properly separated from paper for recycling to avoid impairing the compostability and recyclability of paper [9].

In this context, biopolymers can solve the main environmental constraints and limitations of the food packaging industry [10]. On the one hand, biopolymers can be obtained from natural and renewable sources. On the other hand, the resultant packaging materials can be composted or biodegraded in the environment [11]. Thus, some biopolymers are very promising as paper coating materials, including polysaccharides (e.g., chitosan, starch, lignocellulose derived compounds, and alginates), proteins (e.g., whey, wheat gluten, and zein) and, most relevantly, polyesters such as polylactide (PLA), poly( $\epsilon$ -caprolactone) (PCL), and recently polyhydroxyalkanoates (PHAs) [12]. PHAs are semi-crystalline aliphatic polyesters that offer the advantage of being synthesized by microorganisms using renewable sources, such as sugars and triglycerides, and can also biodegrade under natural conditions [13]. Therefore, PHAs can offer key benefits over petrochemical polymers to reduce packaging's carbon footprint and avoid "white pollution. Poly(3-hydroxybutyrate) (PHB) is the homopolyester and most common type of PHA, which has some physical properties similar to those of PP and PET [14–16]. However, the high crystallinity of PHB results in a highly rigid and brittle material that is also difficult to process due to its narrow processing window and low thermal stability [17,18]. Therefore, the use of microbial copolyesters, for instance poly(3-hydroxybutyrate-co-3-hydroxyvalerate) (PHBV), has been extended [19]. As the comonomer ratio of 3-hydroxyvalerate (3HV) increases in PHBV, the flexibility increases and the melting point is reduced [20,21]. For example, PHBV copolyester with 3HV contents above 10 mol% shows lower crystallinity and a larger processing window [22]. From a mechanical point of view, PHBV is more flexible, ductile, and tough [23]. For example, an increase of 3HV from 0 to 28 mol% significantly improves the elongation at break and impact strength [24]. Thus, the use of PHBV to coat paper represents a highly sustainable strategy to be explored in the packaging field.

The overall objective of this work was to develop and ascertain the performance of paper sheets coated, on both sides, with biodegradable PHBV films by heat sealing. To this end, the variables of the thermo-sealing process for obtaining the multilayers were first analyzed in terms of temperature and time. Then, the multilayers obtained from the most optimized conditions were characterized by their morphology, optical, thermal, mechanical, and vapor and gas barrier properties to determine their suitability for different food preservation applications. The performance of the newly developed multilayers was compared with that of the same paper substrate double coated with a commercial high-barrier multilayer film based on PET and also with that of uncoated paper sheets. Finally, the compostability of the paper sheets was analyzed to estimate the effect of PHBV on the biodegradation and disintegration of paper and, thus, its potential organic recycling.

## 2. Materials and Methods

### 2.1. Materials

Paper sheets with a grammage of  $220 \text{ g}\cdot\text{m}^{-2}$  and thickness of  $290 \mu\text{m}$  were supplied by Billerudkornäs-CrownBoard Prestige™ (Solna, Sweden). According to the manufacturer, this paper derives from 100% wood fibers and is suitable for use in contact with food. A commercial  $10\text{-}\mu\text{m}$  film of PHBV with a 3HV content of 8 mol% was provided by GoodFellow Cambridge Limited (Huntingdon, UK) under the commercial reference BV301010. This grade is also certified by the supplier for its use in contact with food. A  $100\text{-}\mu\text{m}$  high-barrier multilayer film based on PET and EVOH was obtained from Cryovac Inc. (Sealed Air Spain, Buñol, Spain) with commercial reference Cryovac® Darfresh® VST300E TOP WEB. This multilayer film is composed of different petrochemical polymers, but it is herein referred to as PET film for simplicity since it is designed by the manufacturer for PET sealant trays in barrier packaging applications.

*D*-Limonene, with 98% purity, was obtained from Sigma-Aldrich S.A. (Madrid, Spain). Phosphorous pentoxide ( $\text{P}_2\text{O}_5$ ) and magnesium nitrate ( $\text{Mg}(\text{NO}_3)_2$ ) were provided by Panreac Química S.L.U (Castellar del Vallés, Barcelona, Spain). Ripe compost (Abonos Naturales Hnos. Aguado S.L., Toledo, Spain), vermiculite (Leroy Merlin, Valencia, Spain), and microcrystalline cellulose (MCC) (Sigma Aldrich, Madrid, Spain) were used for the biodegradability tests. Refined corn germ oil (Koipe, Córdoba, Spain), sawdust (Productos de limpieza Adrián, Valencia, Spain), saccharose (Azucarera Ebro, Madrid, Spain), rabbit feed (Super Feed S.L., Madrid, Spain), urea (Urea Prill, Antonio Tarazona S.L., Silla, Valencia, Spain), and corn starch (Roquette Laisa, Benifaio, Valencia, Spain) were used for the disintegration tests.

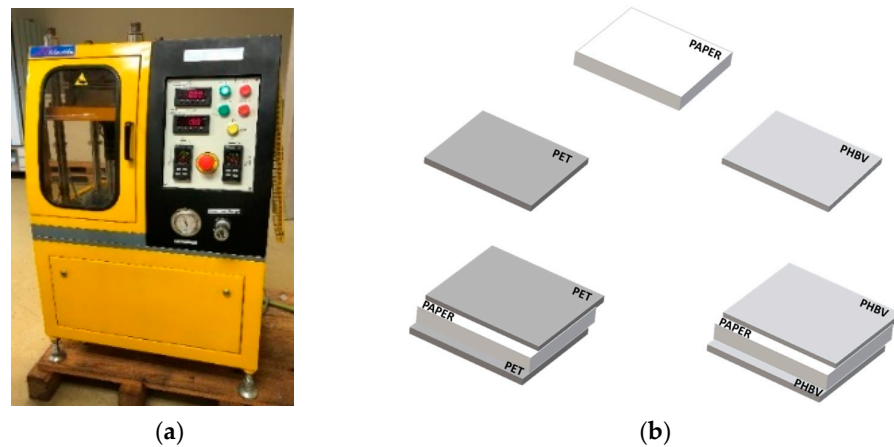
### 2.2. Thermo-Sealing Process

Before preparing the samples, the paper sheets were dried in a vacuum oven (vacuum TEM-TJP Selecta, SA, Barcelona, Spain) at  $60 \text{ }^\circ\text{C}$  for 2 h and, then, stored in a desiccator with  $\text{P}_2\text{O}_5$  (0% RH) at  $25 \text{ }^\circ\text{C}$  until processed. Thereafter, the paper sheets were coated on both sides with PHBV films through a heat-sealing process. For this, the commercial paper sheets and PHBV films were cut in sizes of  $10 \text{ cm} \times 10 \text{ cm}$ . Then, a sheet of paper was placed between two layers of PHBV and subjected to a heat-sealing process in a hydraulic press (Model LP20, Engineering Labtech, Samutprakarn, Thailand). In order to optimize the thermo-sealing process, different temperatures and times were tested. Thus, temperature was increased from  $130$  to  $170 \text{ }^\circ\text{C}$ , in intervals of  $10 \text{ }^\circ\text{C}$  and for periods of 4, 8, 16, and 20 s, maintaining the pressure constant at 20 bar. Thereafter, the multilayers were cooled at room temperature ( $25 \text{ }^\circ\text{C}$ ). The same process was carried out using the multilayer films based on PET at  $160 \text{ }^\circ\text{C}$  for 8 s and a pressure of 20 bar since these conditions were the optimal ones provided by the manufacturer for heat sealing. Figure 1 shows the equipment employed (Figure 1a) and the design of the multilayers (Figure 1b). Finally, the resultant PHBV/paper/PHBV and PET/paper/PET multilayers as well as the as-received uncoated paper sheets were stored in a desiccator with  $\text{P}_2\text{O}_5$  at  $25 \text{ }^\circ\text{C}$  for 15 days prior to characterization. This conditioning was carried out to both adjust the humidity of the samples to dry conditions and to reduce the possible effect of physical aging of PHBV.

### 2.3. Characterization of Multilayer Sheets

#### 2.3.1. Film Thickness

The sheet thickness was measured using a digital micrometer (Palmer model, Comecta S.A., Barcelona, Spain, accuracy of 0.001 mm). Thickness was measured at ten random points, using eight samples for each formulation.



**Figure 1.** (a) Hydraulic press used for the heat-sealing process; (b) scheme of the developed multilayers based on paper sheets and films of poly(3-hydroxybutyrate-co-3-hydroxyvalerate) (PHBV) and polyethylene terephthalate (PET).

### 2.3.2. Optical Evaluation

The internal transmittance ( $T_i$ ) was determined for ascertaining the transparency of the monolayer and multilayer samples by the application of the Kubelka-Munk multiple-scattering theory of the reflection spectrum [25]. This theory is based on the fact that light incident on a translucent material can be absorbed or scattered depending on the material’s absorption ( $K$ ) and scattering ( $S$ ) coefficients. The reflection spectrum ( $R$ ) of the samples from 360 nm to 700 nm was obtained on white ( $R_g$ ) and black ( $R_0$ ) backgrounds using a MINOLTA spectrophotometer (CM-3600d, Minolta Co., Tokyo, Japan). Equations (1) and (2) were used to determine the  $a$  and  $b$  parameters, whereas the reflectance spectra of a sheet with an infinite thickness ( $R_\infty$ ) were calculated according to Equation (3) and  $T_i$  was determined using Equation (4). Three measurements were taken on each sample, at different points, from the glossy side of the paper samples.

$$a = \frac{1}{2} \cdot \left( R + \frac{R_0 - R + R_g}{R_0 \cdot R_g} \right) \tag{1}$$

$$b = \left( a^2 - 1 \right)^{\frac{1}{2}} \tag{2}$$

$$R_\infty = a - b \tag{3}$$

$$T_i = \sqrt{(a - R_0)^2 - b^2} \tag{4}$$

Film color coordinates  $L^*$  ( $L^* = 0$ : black,  $L^* = 100$ : white),  $a^*$  ( $a^* > 0$ : red;  $a^* < 0$ : green), and  $b^*$  ( $b^* > 0$ : yellow;  $b^* < 0$ : blue) were determined from  $R_\infty$  spectra, using  $10^\circ$  observer and D65 illuminant as reference system. The chroma or color saturation ( $C_{ab}^*$ ), expressed from 0 to 100, was determined from Equation (5). The tone or hue angle ( $h_{ab}^*$ ) was calculated from the  $a^*$  and  $b^*$  coordinates, which are expressed in degrees from 0 to  $360^\circ$ , using Equation (6). Finally, Equation (7) was used to determine the color difference ( $\Delta E_{ab}^*$ ), where  $\Delta L^*$ ,  $\Delta a^*$ , and  $\Delta b^*$  correspond to the differences between the color parameters of each multilayer compared to the uncoated paper.

$$C_{ab}^* = \sqrt{a^{*2} + b^{*2}} \tag{5}$$

$$h_{ab}^* = \arctg\left(\frac{b^*}{a^*}\right) \tag{6}$$

$$\Delta E^* = \sqrt{(\Delta L^*)^2 + (\Delta a^*)^2 + (\Delta b^*)^2} \tag{7}$$

The color change was evaluated according to the following criteria: negligible ( $\Delta E_{ab}^* < 1$ ), only an experienced observer can tell the difference ( $\Delta E_{ab}^* \geq 1$  and  $< 2$ ); an inexperienced observer notes the difference ( $\Delta E_{ab}^* \geq 2$  and  $< 3.5$ ); there is a clear notable difference ( $\Delta E_{ab}^* \geq 3.5$  and  $< 5$ ); and the observer notices different colors ( $\Delta E_{ab}^* \geq 5$ ) [26].

### 2.3.3. Microstructural Analysis

The cross-sections of the monolayers and multilayers were obtained by immersion and cryo-fracture in liquid nitrogen. The samples were mounted, using double-sided carbon tape, on the observation holders and covered with a platinum layer (EM MED020 sputter coater, Leica Biosystems, Barcelona, Spain). The cross-sections were then observed by Field Emission Scanning Electron Microscopy (FESEM) in a JEOL model JSM-5410 (Tokyo, Japan), operating at 2.0 kV acceleration voltage. The thicknesses of the internal layers of the samples were determined using the ImageJ v1.53c Program.

### 2.3.4. Thermal Analysis

The thermal behavior of the different monolayers and multilayers was analyzed by thermogravimetric analysis (TGA) in a TGA 1 Stare System analyzer (Mettler-Toledo GmbH, Greifensee, Switzerland). Approximately 5 mg of the conditioned samples were placed in an alumina pan and heated from 25 to 800 °C at 10 °C·min<sup>-1</sup> in inert atmosphere under a nitrogen flow-rate of 10 mL·min<sup>-1</sup>. From the TGA curves and their derivative curves (DTG), the corresponding  $T_{\text{onset}}$  values (temperature at which thermal degradation begins, corresponding to 5% mass loss),  $T_{\text{deg}}$  (temperature at maximum degradation rate), percentage of mass lost when the  $T_{\text{deg}}$  is reached, and percentage of mass remaining at 800 °C were determined. The analysis was performed in duplicate for each formulation.

### 2.3.5. Tensile Tests

The tensile properties of the samples were determined using a universal testing machine (Stable Micro System TA-XT plus, Haslemere, UK) following the standard method ASTM D882 [27]. To this end, the pre-conditioned samples, previously cut in dimensions of 25 mm × 100 mm, were stretched by two grips, initially separated by 100 mm, at a crosshead speed of 50 mm·min<sup>-1</sup> until breakage (model A/TG, Stable Micro System, Haslemere, UK). Stress ( $\sigma$ ) versus strain ( $\epsilon$ ) curves were obtained from the force-distance curves by considering sample dimensions and degree of deformation. The Young's modulus (E), stress at yield or elastic limit ( $\sigma_y$ ), and percentage of elongation at break (%  $\epsilon_b$ ) were obtained. Eight samples for each formulation were analyzed.

### 2.3.6. Permeability Measurements

Permeances to water and limonene vapors of the monolayers and multilayers were determined at 25 °C and 53% RH by the gravimetric methodology according to ASTM E96/E96M [28]. For water vapor, the film and sheet samples ( $\varnothing = 3.5$  cm) were placed and sealed in Payne permeability cups filled with 5 mL of distilled water (100% RH). Then, the cups were placed into desiccators containing an  $\text{Mg}(\text{NO}_3)_2$  oversaturated solution and, for one week, weighed periodically (ME36S,  $\pm 0.00001$  g accuracy, Sartorius, Goettingen, Germany). The water vapor permeance was calculated from the water vapor transmission rate (WVTR), determined from the slope of the weight loss vs. time, and corrected for permeant partial pressure. In the case of limonene vapor, the procedure was similar to that described for water vapor but using 5 mL of D-limonene instead of water. Thus, limonene permeation rate (LPR) was obtained from the steady-state permeation slopes of weight loss vs. time and corrected for permeant partial pressure. In both cases, cups with aluminum films were used as control samples to estimate and subtract the vapor loss through the sealing. All the vapor permeance measurements were performed in triplicate.

The oxygen permeance of the monolayers and multilayers was determined using an oxygen permeation analyzer (OxySense<sup>®</sup> Model 8101e, Systech Illinois, Thame, UK) at 25 °C and 53% RH according to ASTM D3985-05 [29]. The exposed sample area was 50 cm<sup>2</sup>

and the permeance values were derived from the oxygen transmission rate (OTR) measurements, which were corrected with the gas partial pressure and recorded in triplicate.

#### 2.4. Controlled Composting Tests

##### 2.4.1. Aerobic Biodegradability

The aerobic biodegradability of the monolayers and multilayers was determined under composting conditions by measuring the amount of CO<sub>2</sub> generated according to ISO 14855 [30]. The ripe compost was mixed with vermiculite (compost/vermiculite ratio: 3:1) to avoid compaction of the compost and to ensure good oxygen access. Glass flasks (2L) containing two PP flasks (60 mL) were used as reactors. One of the flasks contained 3 g of dry compost mixed with 1 g of vermiculite and an amount of sample (previously cut into 2 mm<sup>2</sup> squares) equivalent to 50 mg of carbon, while the other flask contained deionized water to ensure 100% RH. The bioreactors were closed and incubated for 45 days at 58 ± 2 °C. One reactor containing only compost was used as blank and one reactor containing MCC mixed with the compost were used as reference sample. The percentage of CO<sub>2</sub> generated inside the reactors was measured, in triplicate, using a CO<sub>2</sub> analyzer (Gaspac Advance Micro GS3, Systech Illinois, Thame, UK) throughout the biodegradation process. The percentage of biodegradation was calculated using the following Equation (8), assuming that all the carbon in the sample was converted into CO<sub>2</sub>:

$$B(\%) = \frac{\sum CO_{2S} - \sum CO_{2B}}{CO_2^{ThS}} \times 100 \quad (8)$$

where  $\sum CO_{2S}$  is the accumulative amount of CO<sub>2</sub> produced in the sample bioreactor,  $\sum CO_{2B}$  is the accumulative amount of CO<sub>2</sub> produced in the blank bioreactor, and  $CO_2^{ThS}$  is the theoretical amount of CO<sub>2</sub> that the test material can produce.

##### 2.4.2. Degree of Disintegration

Disintegration of the monolayers and multilayers in simulated composting conditions was conducted at 58 ± 2 °C and 55% RH to ensure controlled thermophilic conditions, as indicated by ISO 20200 [31]. Film samples sizing 25 mm × 25 mm were placed in mesh bags (1 mm × 1 mm mesh size) and buried in a controlled soil compost made of sawdust (40 wt%), rabbit feed (30 wt%), ripe compost (10 wt%), corn starch (10 wt%), sucrose (5 wt%), corn seed oil (4 wt%), and urea (1 wt%). Samples were periodically unburied from the composting facility. At the initial time and throughout the study, the reactors were weighed and deionized water was added, if necessary, to restore the initial mass, as specified by the standard [31]. Thus, mesh bags, each with one sample square, were extracted from the reactor at different control times in order to carry out the visual morphological analysis and determine mass loss. To this end, the mesh bags containing samples were dried, gently cleaned with a soft brush to eliminate the adhered compost residues, and weighed with an analytical balance. The analysis was conducted for 300 days to ascertain the effect on paper disintegration of the biopolymer coatings for long periods. The weight loss was calculated using Equation (9):

$$Weight\ loss\ (\%) = \frac{W_0 - W_t}{W_0} \times 100 \quad (9)$$

where  $W_0$  is the initial dry weight of the sample and  $W_t$  is the weight of the sample after a bury time  $t$ . All tests were carried out in triplicate to ensure reliability.

#### 2.5. Statistical Analysis

The experimental data were submitted to analysis of variance (ANOVA) using Statgraphics Centurion XVI software (Manugistics Corp., Rockville, MD, USA). Fisher's least significant difference (LSD) procedure was used at the 95% confidence level.

### 3. Results

#### 3.1. Development of Paper Multilayers

The results of the application of different time and temperature conditions to form the PHBV/paper/PHBV multilayer sheets during the heat-sealing process are shown in Table 1. It gathers the set of values of temperature and time employed to produce the multilayers, ranging from 130 °C to 170 °C and 4 to 20 s, respectively. It also includes an image of the surface of the PHBV/paper/PHBV multilayer attained at each condition, with comments on the quality and/or processing aspects. It can be seen that the application of very low temperatures, that is, 130 °C, was not high enough for heat sealing of the PHBV films on the paper sheet, even if applied for long times, of up to 20 s. Interestingly, increasing the temperature to 140 °C significantly improved the heat-sealability of the PHBV films on the paper substrate. However, for this temperature, processing times of at least 8 s were necessary to obtain uniformity and good adhesion between the substrates and coatings. Moreover, the application of heat-sealing temperatures of 150 °C also resulted in good adhesion between the layers, but the resultant multilayers presented areas full of wrinkles and bubbles. The latter effect can be related to occluded air or evaporated water produced by the effect of high temperature on the paper substrate, which is a very hydrophilic material based on cellulose fibers. Therefore, despite having worked with dried samples, the paper sheets could retain minimal amounts of water and/or adsorbed moisture during handling and processing. As the sealing processing time increased, these effects occurred to a greater extent. Finally, the use of the highest temperatures, and especially at 170 °C, resulted in the partial melting of the PHBV film and a subsequent deterioration of the heat-sealed multilayers, even at short processing times. In this regard, it should be noted that the melting temperature of PHBV copolyesters with 3HV contents of up to 20 %mol ranges from approximately 154 °C to 171 °C [32].

**Table 1.** Optimization of the thermo-sealing process of the poly(3-hydroxybutyrate-co-3-hydroxyvalerate) (PHBV) films on both sides of paper.

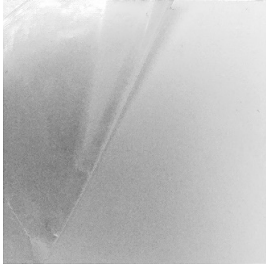
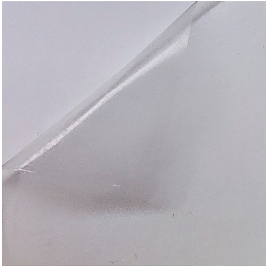
Temperature (°C)	Time (s)	Multilayer	Comments
130	4		The PHBV film and paper sheet did not stick properly.
	8		The PHBV film detached easily from the paper sheet.

Table 1. Cont.

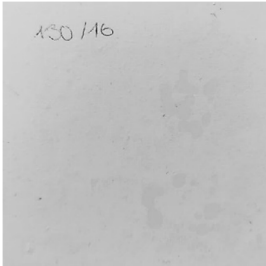
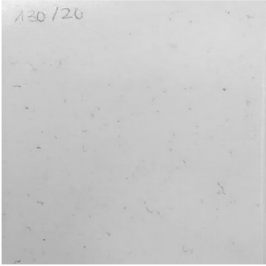
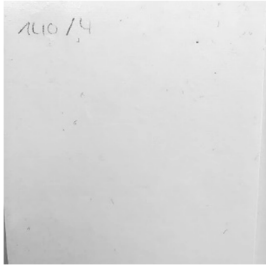
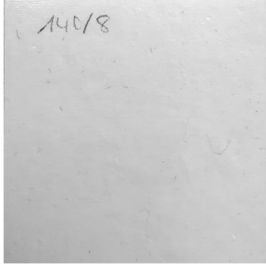
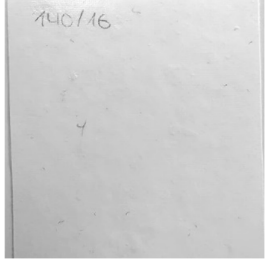
Temperature (°C)	Time (s)	Multilayer	Comments
	16		The multilayer was homogenous but the PHBV film and paper sheet detached easily.
	20		The multilayer showed some opaque areas where the PHBV film was not properly adhered to paper.
	4		The PHBV film and the paper sheet sealed, but presented poor adhesion in some areas.
140	8		The PHBV film and the paper sheet sealed properly.
	16		The PHBV film and the paper sheet sealed properly.



Table 1. Cont.

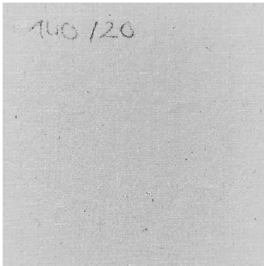
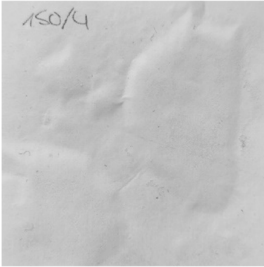

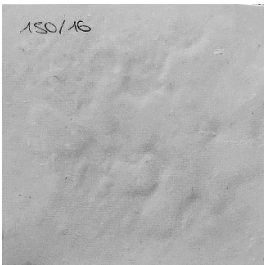
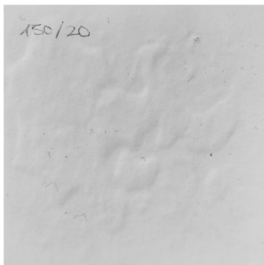
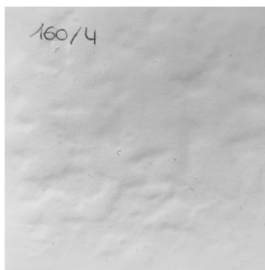
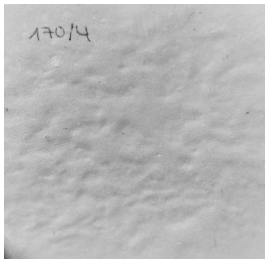
Temperature (°C)	Time (s)	Multilayer	Comments
150	20		The PHBV film and the paper sheet sealed properly.
	4		The PHBV film and paper sheet sealed, but the multilayer showed large areas with wrinkles and bubbles due to occluded air or moisture.
	8		The PHBV film and paper sheet sealed, but the multilayer showed large areas with wrinkles and bubbles due to occluded air or moisture.
	16		The PHBV film and paper sheet remained sealed, but the multilayer still presented several wrinkles and bubbles.
	20		The PHBV film and paper sheet remained sealed and the surface of the multilayer improved, but it still presented some wrinkles and bubbles.

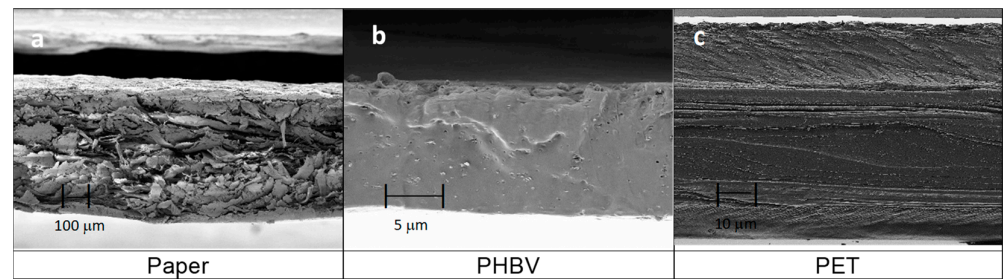
Table 1. Cont.

Temperature (°C)	Time (s)	Multilayer	Comments
160	4		The PHBV film partially melted in several areas and the surface still showed some wrinkles and bubbles. Further times at this temperature were ruled out of the study.
170	4		The PHBV film partially melted in several areas and the film still showed some wrinkles and bubbles. Further temperatures and times were ruled out of the study.

Based on the results obtained from the heat-sealing process, it was concluded that the optimal conditions were obtained at a temperature of 140 °C, with times ranging between 8 and 20 s. Since no improvement was observed for times longer than 8 s, the shortest time was selected to minimize costs and reduce energy consumption. Therefore, the heat-sealing process of the PHBV/paper/PHBV multilayers was set at 140 °C and 8 s.

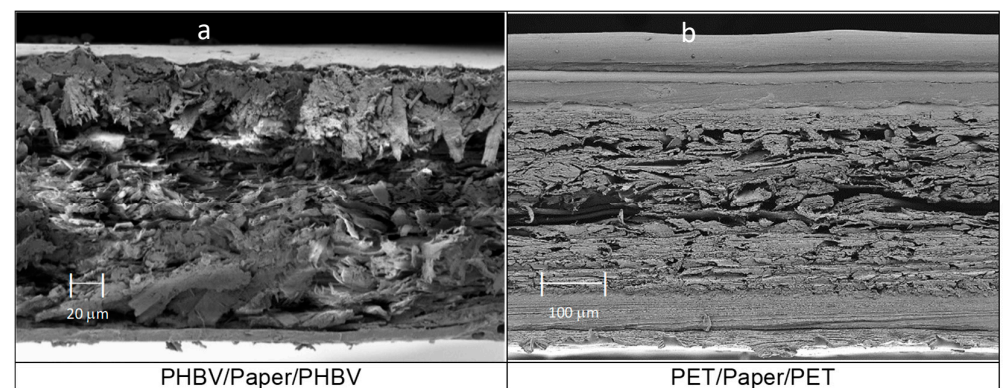
### 3.2. Morphology of Paper Multilayers

Figure 2 shows the cross-sectional morphology observed by FESEM of the three components of the multilayers, that is, the paper sheet and the PHBV and PET films. As can be seen in Figure 2a, the paper sheet presented an average thickness of  $291 \pm 6 \mu\text{m}$  and it was composed of micrometer-sized fibers, giving rise to a cross-section with a rough surface. These cellulosic fibers, which showed an average diameter of approximately  $20 \mu\text{m}$ , are responsible for the high level of porosity of the paper [33]. In contrast, one can observe in Figure 2b that the PHBV film showed a continuous section of  $12 \pm 2 \mu\text{m}$ , with a brittle fracture, because there were no macroscopic plastic deformations. The observed inorganic microparticles embedded in the biopolymer matrix may correspond to boron nitride, which is habitually employed by the manufacturer as a nucleating agent during the fabrication of PHAs [34]. Finally, Figure 2c shows the section of the commercial PET film, which presented a multilayer structure having an average thickness of  $104 \pm 1 \mu\text{m}$ . The external layer, shown at the bottom with a lower thickness, can be ascribed to a sealing layer of polyolefin (e.g., LDPE or PP) or a modified PET (e.g., polyethylene terephthalate glycol, PET-G) with a low sealing temperature. Both the thickest internal layer and the upper external layer would correspond to PET. Moreover, the inner layers with low thickness can be related to EVOH. The layer structure attributed herein is based on that previously observed for a polyolefin-based multilayer, supplied by the same manufacturer for this product range (Cryovac® Darfresh® VST200P TOP WEB), which contained two inner layers of EVOH of nearly  $5 \mu\text{m}$  to provide the film with high oxygen barrier capacity [35].



**Figure 2.** Field emission scanning electron microscopy (FESEM) micrographs taken in the cross-sections of: (a) paper sheet, observed at 150 $\times$ ; (b) poly(3-hydroxybutyrate-co-3-hydroxyvalerate) (PHBV) film, at 3000; (c) multilayer film based on polyethylene terephthalate (PET), at 750 $\times$ .

On the other hand, Figure 3 shows the morphology of the paper-based multilayer structures obtained from the different monolayers, presented in Figure 2, by the heat-sealing process. Thus, Figure 3a shows the resultant three-layer structure based on the paper substrate coated, on both sides, with PHBV films. The average thickness of the multilayer sheet, measured after heat sealing, resulted in a value of  $297 \pm 8 \mu\text{m}$ . Likewise, a similar morphology was observed for the paper coated by two PET-based multilayer films, the so-called PET/paper/PET sheet, shown in Figure 3b. This multilayer sheet presented an analogous structure with a higher average thickness, of  $473 \pm 3 \mu\text{m}$ , due to the higher thickness of the outer layers of the PET-based films. Both multilayer sheets, that is, PHBV/paper/PHBV and PET/paper/PET, showed good adhesion between the polyester layers and paper substrate, suggesting adequate mechanical resistance for handling and transport in food packaging. Furthermore, it is also worth noting that both multilayers were slightly thinner than the sum of the thicknesses of the individual monolayers. This is due to the radial flow of the polyester monolayers and to the reduction of the free volume of the paper (highly porous) during the heat-sealing step.

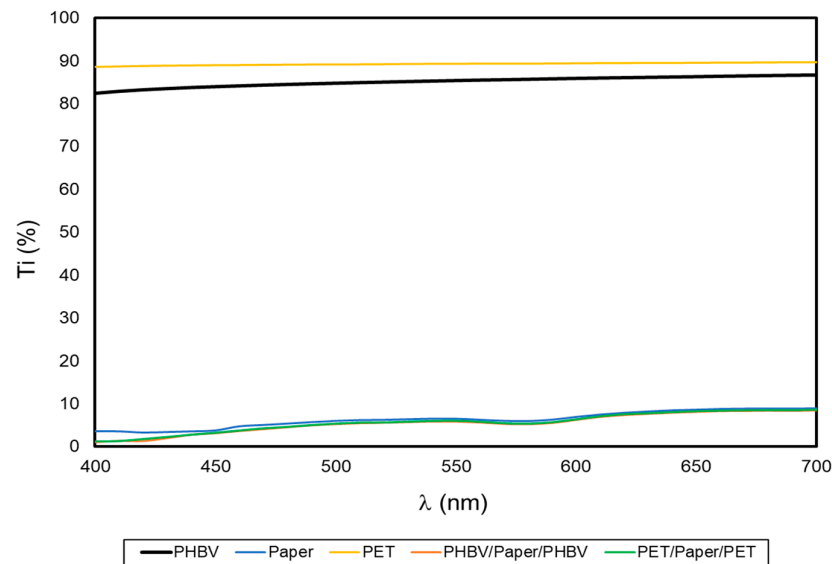


**Figure 3.** Field emission scanning electron microscopy (FESEM) micrographs taken in the cross-sections of: (a) poly(3-hydroxybutyrate-co-3-hydroxyvalerate) (PHBV)/Paper/PHBV multilayer sheet, taken at 200 $\times$ ; (b) polyethylene terephthalate (PET)/Paper/PET multilayer sheet, at 150 $\times$ .

### 3.3. Optical Properties of Paper Multilayers

One of the desired characteristics of packaging materials is that these should protect food from the effects of light, especially ultraviolet (UV) radiation, which is one of the main benefits of paper. Figure 4 shows the spectral distribution curves that represent  $T_i$  of the film and sheet samples as a function of the wavelength ( $\lambda$ ). Thus, high  $T_i$  values are related to high light transmittance of the samples and, therefore, correspond to more transparent films or sheets while, as opposite, low  $T_i$  values are related to more opaque samples with lower light passage [36,37]. As can be seen in the graph, both PHBV and PET films presented notably higher  $T_i$  values (in agreement with their high transparency) compared to the uncoated paper and multilayer sheets. The slightly lower  $T_i$  of the PHBV

film compared with the PET multilayer film can be related to the higher crystallinity of the microbial copolyester [38]. As expected, the coating of the paper sheets did not affect the paper's opacity, thus confirming that the good barrier against light was preserved. This may be of interest for the protection of certain foods, such as oil or meat, that must be protected against light-induced oxidative processes [39].



**Figure 4.** Spectral distribution curves of the percentage internal transmittance (%  $T_i$ ) of the paper sheet, poly(3-hydroxybutyrate-co-3-hydroxyvalerate) (PHBV) and polyethylene terephthalate (PET) films, and PHBV/paper/PHBV and PET/paper/PET multilayer sheets.

Table 2 shows the values of the optical properties of the film and sheet samples. The uncoated paper and paper multilayer sheets presented similar high  $L^*$  values, 95–96, while the neat PHBV and PET films showed lower values, 91–92. No remarkable differences were found in the color parameters of the polyester films, with both exhibiting high film lightness in agreement with previous studies [40,41]. Likewise, no significant differences ( $p > 0.05$ ) were found among the  $L^*$  values of the paper multilayers and the uncoated paper, so the presence of the polyester films did not alter the lightness of the paper sheets. Nevertheless, multilayers exhibited more bluish (lower  $h_{ab}^*$  values) and less saturated (lower  $C_{ab}^*$  values) color in comparison with the uncoated paper sample. Nevertheless, these differences, calculated through  $\Delta E_{ab}^*$  parameter, were not relevant from a practical point of view since color differences below 2 are hardly perceived by the human eye [42].

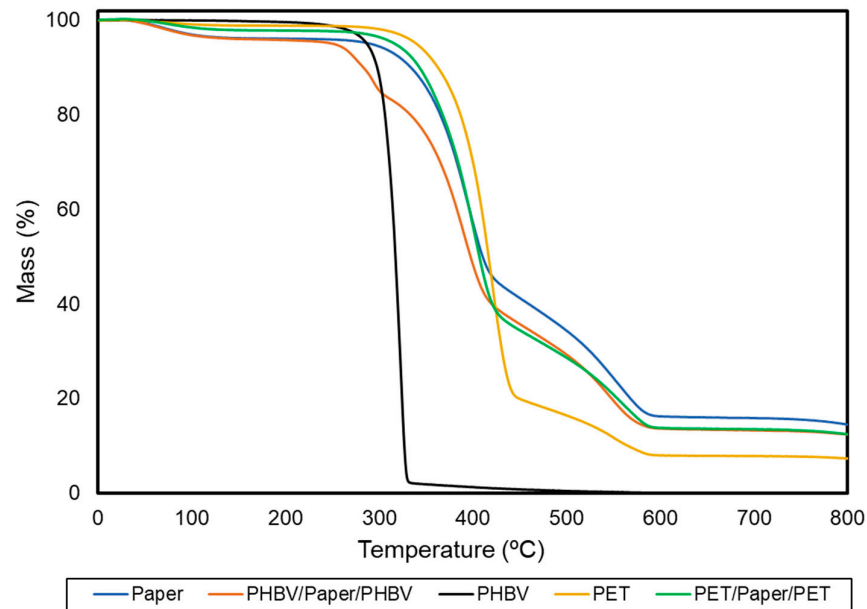
**Table 2.** Color parameters in terms of lightness ( $L^*$ ), color coordinates ( $a^*$  and  $b^*$ ), chroma ( $C_{ab}^*$ ), hue ( $h_{ab}^*$ ), and total color difference ( $\Delta E_{ab}^*$ ) of the paper sheet, poly(3-hydroxybutyrate-co-3-hydroxyvalerate) (PHBV) and polyethylene terephthalate (PET) films, and PHBV/paper/PHBV and PET/paper/PET multilayer sheets.

Sample	$L^*$	$a^*$	$b^*$	$C_{ab}^*$	$h_{ab}^*$	$\Delta E_{ab}^*$
Paper	95.80 ± 0.03 <sup>a</sup>	1.36 ± 0.05 <sup>a</sup>	−5.39 ± 0.20 <sup>a</sup>	5.55 ± 0.21 <sup>a</sup>	284.21 ± 0.09 <sup>a</sup>	-
PHBV	91.40 ± 0.02 <sup>b</sup>	−0.37 ± 0.01 <sup>b</sup>	1.87 ± 0.06 <sup>b</sup>	1.91 ± 0.06 <sup>b</sup>	101.25 ± 0.06 <sup>b</sup>	-
PET	91.59 ± 0.06 <sup>b</sup>	−0.36 ± 0.01 <sup>b</sup>	1.64 ± 0.01 <sup>bc</sup>	1.68 ± 0.01 <sup>c</sup>	102.59 ± 0.01 <sup>c</sup>	-
PHBV/Paper/PHBV	95.54 ± 0.06 <sup>a</sup>	0.75 ± 0.09 <sup>c</sup>	−3.66 ± 0.30 <sup>d</sup>	3.73 ± 0.31 <sup>d</sup>	281.61 ± 0.53 <sup>d</sup>	1.85 ± 0.06 <sup>a</sup>
PET/Paper/PET	95.52 ± 0.05 <sup>a</sup>	0.86 ± 0.02 <sup>cd</sup>	−3.56 ± 0.14 <sup>d</sup>	3.66 ± 0.14 <sup>d</sup>	283.63 ± 0.30 <sup>e</sup>	1.92 ± 0.07 <sup>a</sup>

Mean values and standard deviation. <sup>a–e</sup> Different superscripts in the same column indicate significant differences between formulations ( $p < 0.05$ ).

### 3.4. Thermal Properties of Paper Multilayers

Thermal stability was determined by TGA to ascertain the application conditions of the resultant multilayer sheets. The TGA curves of each sample, which show the variation of the mass percentage as a function of temperature, are gathered in Figure 5. Table 3 includes the resultant thermal stability parameters.



**Figure 5.** Thermogravimetric analysis (TGA) curves of the paper sheet, poly(3-hydroxybutyrate-co-3-hydroxyvalerate) (PHBV) and polyethylene terephthalate (PET) films, and PHBV/paper/PHBV and PET/paper/PET multilayer sheets.

**Table 3.** Thermal properties in terms of temperature at which thermal degradation begins ( $T_{onset}$ ), corresponding to 5% mass loss, temperature of maximum degradation rate ( $T_{deg}$ ), percentage of mass loss at  $T_{deg}$ , and percentage of remaining mass at 800 °C of the paper sheet, poly(3-hydroxybutyrate-co-3-hydroxyvalerate) (PHBV) and polyethylene terephthalate (PET) films, and PHBV/paper/PHBV and PET/paper/PET multilayer sheets.

Sample	$T_{onset}$ (°C)	$T_{deg}$ (°C)	Mass Loss at $T_{deg}$ (%)	Remaining Mass (%)
Paper	310.8 ± 7.8 <sup>a</sup>	353.8 ± 1.6 <sup>a</sup>	39.4 ± 1.0 <sup>a</sup>	14.0 ± 0.1 <sup>a</sup>
PHBV	289.7 ± 5.2 <sup>b</sup>	288.2 ± 3.8 <sup>b</sup>	60.6 ± 0.5 <sup>b</sup>	0.1 ± 0.0 <sup>b</sup>
PET	327.3 ± 3.7 <sup>c</sup>	367.5 ± 3.2 <sup>c</sup>	49.1 ± 8.9 <sup>c</sup>	7.2 ± 0.8 <sup>c</sup>
PHBV/Paper/PHBV	275.5 ± 4.3 <sup>d</sup>	349.6 ± 2.9 <sup>d</sup>	54.8 ± 0.2 <sup>d</sup>	12.0 ± 1.6 <sup>d</sup>
PET/Paper/PET	313.6 ± 4.1 <sup>a</sup>	357.9 ± 1.1 <sup>e</sup>	55.2 ± 0.4 <sup>d</sup>	11.4 ± 0.9 <sup>d</sup>

Mean values and standard deviation. <sup>a–e</sup> Different superscripts in the same column indicate significant differences between formulations ( $p < 0.05$ ).

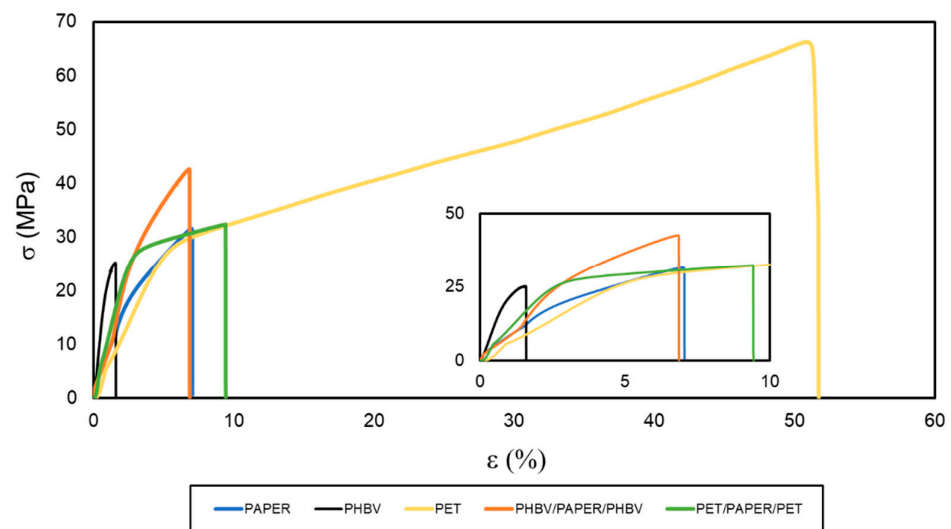
In the case of paper, three relevant mass losses occurred during heating, which approximately took place at temperatures of 100, 350, and 490 °C. These mass losses have been widely studied in lignocellulosic materials [43]. The first one corresponds to the evaporation of absorbed water in the dried paper sheets, which indicates that the initial moisture content of these samples was 2–3%. The second and main degradation step, between 310 and 410 °C, showed an average mass loss of nearly 55%. This is referred to as the “active pyrolysis zone” since the mass loss rate is high. This mass loss corresponds to the decomposition of hemicellulose and cellulose, which are main components of paper. Both degradation processes are known to involve complex reactions (e.g., dehydration and decarboxylation, among others) as well as the breaking of C–H, C–O, and C–C

bonds [44]. The onset of the third stage of degradation overlapped with the previous one and continued progressively until temperatures neared 600 °C. In this step, the mass loss was around 28%, representing the “passive pyrolysis zone” since the mass loss rate was much lower than that observed in the previous one. The latter mass loss can be assigned to the thermal decomposition of lignin, which is known to occur slowly and over a wide temperature range. Furthermore, at 800 °C, the paper showed a remaining mass of 14%. This mass corresponds to both inorganic material, such as silica or titanium dioxide (TiO<sub>2</sub>), which is usually applied to give brightness and whiteness to paper, and ashes generated from the decomposition of the organic material in an inert atmosphere [45].

Furthermore, PHBV thermal degradation occurred through a single and sharp degradation step that occurred from 290 to 320 °C. Thermal degradation of PHAs generally follows a random chain scission model of the ester bond, involving a cis-type elimination reaction of –CH and a six-membered ring transition to form crotonic acid and oligomers [46]. The thermal stability of the PET film was significantly higher ( $p < 0.05$ ) than that of PHBV. This thermal degradation occurred in two stages. The first one occurred in the 300–450 °C range that corresponds to the degradation of the polymer chains. The second one was seen between 450 and 600 °C and it is due to the thermo-oxidative degradation of the residual mass produced during the first stage. This thermal degradation of PET is based on a heterolytic cleavage by means of a six-membered intermediate ring. In this process, the hydrogen of a beta (β)-carbon of the ester group is transferred to the carbonyl group of the ester, followed by a breakage of the ester bonds [47]. Whereas the application of the PET films on the paper substrate slightly improved its thermal stability ( $p > 0.05$ ), the thermal resistance of the PHBV/paper/PHBV multilayer slightly but significantly ( $p < 0.05$ ) decreased. In particular, a reduction of around 11% in comparison with the uncoated paper was observed. The latter effect is due to the lower thermal stability of the biopolyester. Nevertheless, the thermal stability of the PHBV/paper/PHBV multilayer can be yet considered adequate for most food packaging applications that do not exceed temperatures above 250 °C, such as microwave heating. In contrast, most heating processes in the oven will be restricted, where the use of neat paper is still very limited [48].

### 3.5. Mechanical Properties of Paper Multilayers

The mechanical performance of the multilayers was studied by means of tensile tests at room temperature. The resultant  $\sigma$  versus  $\epsilon$  curves are shown in Figure 6. The most characteristic values, namely  $E$ ,  $\sigma_y$ , and  $\epsilon_b$ , obtained from these curves, are included in Table 4. It can be observed that the paper sheet showed mechanical parameters that correspond to a rigid and brittle material. This sample broke right after exceeding the elastic deformation zone, with a  $\sigma_y$  value of 31.9 MPa and deformations of nearly 7%. Moreover, the PHBV film also showed a brittle behavior, but it was significantly ( $p < 0.05$ ) more rigid than the paper sample due to its higher value of  $E$ , 2928 MPa. The high brittleness of PHBV derives from its high crystallinity, even though the 3HV content in the copolyester was relatively high (10 mol%). This embrittlement takes place by a process of secondary crystallization and/or physical aging that results in the formation of large spherulites acting as stress concentration points [21]. The mechanical behavior of the PET film followed a completely different pattern, being typical of a more stretchable and ductile material. This film sample showed  $E$  and  $\sigma_y$  values of approximately 759 and 29.6 MPa, respectively, and broke at a deformation of nearly 53% with a maximum strength above 60 MPa. This mechanical behavior is in agreement with the values reported for PET films in a previous study [9].



**Figure 6.** Stress ( $\sigma$ ) versus strain ( $\epsilon$ ) curves of the paper sheet, poly(3-hydroxybutyrate-co-3-hydroxyvalerate) (PHBV) and polyethylene terephthalate (PET) films, and PHBV/paper/PHBV and PET/paper/PET multilayer sheets.

**Table 4.** Mechanical properties in terms of Young's modulus (E), stress at yield ( $\sigma_y$ ), and percentage of elongation at break (%  $\epsilon_b$ ) of the paper sheet, poly(3-hydroxybutyrate-co-3-hydroxyvalerate) (PHBV) and polyethylene terephthalate (PET) films, and PHBV/paper/PHBV and PET/paper/PET multilayer sheets.

Sample	E (MPa)	$\sigma_y$ (MPa)	$\epsilon_b$ (%)
Paper	1787 $\pm$ 41 <sup>a</sup>	31.9 $\pm$ 1.0 <sup>a</sup>	6.9 $\pm$ 0.9 <sup>a</sup>
PHBV	2928 $\pm$ 30 <sup>b</sup>	27.0 $\pm$ 2.8 <sup>b</sup>	2.3 $\pm$ 0.6 <sup>b</sup>
PET	759 $\pm$ 18 <sup>c</sup>	29.6 $\pm$ 2.1 <sup>c</sup>	52.8 $\pm$ 0.6 <sup>c</sup>
PHBV/Paper/PHBV	2591 $\pm$ 51 <sup>d</sup>	43.2 $\pm$ 2.1 <sup>d</sup>	7.1 $\pm$ 1.2 <sup>a</sup>
PET/Paper/PET	1959 $\pm$ 20 <sup>e</sup>	29.4 $\pm$ 2.3 <sup>c</sup>	9.8 $\pm$ 0.9 <sup>d</sup>

Mean values and standard deviation. <sup>a-e</sup> Different superscripts in the same column indicate significant differences between formulations ( $p < 0.05$ ).

Double coating led to a significant enhancement of the tensile properties of the paper substrate, which significantly ( $p < 0.05$ ) depended on the type of polyester used. In the case of the PHBV/paper/PHBV multilayer, it gave rise to a sheet with an E of 2591 MPa and an  $\sigma_y$  of approximately 43 MPa. Thus, the PHBV double coating yielded an improvement in terms of mechanical resistance when compared with the uncoated paper substrate, without affecting significantly ( $p > 0.05$ ) ductility ( $\epsilon_b$  of 7.1%). Similarly, for the PET/paper/PET multilayer, values of E of 1959 MPa and  $\sigma_y$  of 29.4 MPa were obtained. However, this multilayer sample broke at deformation values of approximately 10%, indicating a significant improvement ( $p < 0.05$ ) in the flexible properties of paper. In this sense, it is also worth mentioning that, although both films were notably thinner than paper, the PET film used was approximately 10 times thicker than the PHBV film so that the proportion of petrochemical film in the multilayer with respect to paper was higher than in the case of the biopolyester film. Therefore, the PHBV/paper/PHBV multilayer yielded to a greater mechanical resistance, while the PET/paper/PET multilayer was more stretchable than the uncoated paper. According to these results, in terms of food packaging applications, the newly developed PHBV/paper/PHBV multilayers will be mainly restricted to rigid applications. For example, these can be applied to develop trays, lids, or plates, which do not require high deformations but can withstand certain stresses.

### 3.6. Barrier Properties of Paper Multilayers

The permeance values of the water and limonene vapors and oxygen gas of the uncoated paper sheet, PHBV and PET films, and multilayer paper sheets are shown in Table 5. Permeance is the expression of permeability with the removal of the thickness factor, used to determine the barrier of multilayer structures and the actual performance of a film at given conditions of temperature and %RH. For this reason, the thickness values of each film and sheet samples were also included.

**Table 5.** Permeance to water and D-limonene vapors and oxygen of the paper sheet, poly(3-hydroxybutyrate-co-3-hydroxyvalerate) (PHBV) and polyethylene terephthalate (PET) films, and PHBV/paper/PHBV and PET/paper/PET multilayer sheets.

Sample	Thickness ( $\mu\text{m}$ )	Water Vapor		Limonene Vapor		Oxygen	
		Permeance $\times 10^{10}$ ( $\text{kg}/\text{m}^2 \cdot \text{Pa} \cdot \text{s}$ )	Permeability $\times 10^{15}$ ( $\text{kg} \cdot \text{m}/\text{m}^2 \cdot \text{Pa} \cdot \text{s}$ )	Permeance $\times 10^{10}$ ( $\text{kg}/\text{m}^2 \cdot \text{Pa} \cdot \text{s}$ )	Permeability $\times 10^{15}$ ( $\text{kg} \cdot \text{m}/\text{m}^2 \cdot \text{Pa} \cdot \text{s}$ )	Permeance $\times 10^{15}$ ( $\text{m}^3/\text{m}^2 \cdot \text{Pa} \cdot \text{s}$ )	Permeability $\times 10^{19}$ ( $\text{m}^3 \cdot \text{m}/\text{m}^2 \cdot \text{Pa} \cdot \text{s}$ )
Paper	$291 \pm 6^a$	$110 \pm 9^a$	$3205 \pm 87^a$	$22.3 \pm 1.3^a$	$650 \pm 9^a$	> D.L.	> D.L.
PHBV	$12 \pm 2^b$	$4.8 \pm 0.7^b$	$5.7 \pm 0.3^c$	$5.8 \pm 0.3^b$	$6.95 \pm 0.14^c$	$24.1 \pm 5^a$	$2.89 \pm 0.17^a$
PET *	$104 \pm 1^a$	$0.23 \pm 0.04^d$	$2.3 \pm 0.4^d$	$0.49 \pm 0.01^e$	$4.97 \pm 0.14^d$	$0.81 \pm 0.01^b$	$0.86 \pm 0.17^b$
PHBV/Paper/PHBV	$297 \pm 8^c$	$4.5 \pm 0.8^c$	-	$4.4 \pm 0.8^c$	-	$3.4 \pm 0.8^c$	-
PET/Paper/PET	$473 \pm 3^d$	$0.19 \pm 0.01^d$	-	$0.8 \pm 0.2^d$	-	$0.14 \pm 0.01^b$	-

\* Assuming a monolayer material. Mean values and standard deviation. <sup>a-e</sup> Different superscripts in the same column indicate significant differences between formulations ( $p < 0.05$ ).

Regarding the water vapor, one can observe that the permeance of the paper sheet was  $1.10 \times 10^{-8} \text{ kg}/\text{m}^2 \cdot \text{Pa} \cdot \text{s}$ , resulting in a permeability value of  $3.21 \times 10^{-12} \text{ kg} \cdot \text{m}/\text{m}^2 \cdot \text{Pa} \cdot \text{s}$ . The low water vapor barrier of paper is due to the fact that it is a hydrophilic and highly fibrous material and, therefore, has a high porosity, as observed previously during the FESEM analysis. In relation to the 10- $\mu\text{m}$  PHBV film, it presented a permeance of  $4.78 \times 10^{-10} \text{ kg}/\text{m}^2 \cdot \text{Pa} \cdot \text{s}$ , yielding a permeability of  $5.73 \times 10^{-15} \text{ kg} \cdot \text{m}/\text{m}^2 \cdot \text{Pa} \cdot \text{s}$ . This permeability value is slightly higher than that reported for thermo-compressed films of PHB [49] and PHBV with 2–3 mol% 3HV [50], that is,  $1.70$  and  $1.82 \times 10^{-15} \text{ kg} \cdot \text{m}/\text{m}^2 \cdot \text{Pa} \cdot \text{s}$ , respectively. This difference is due to the higher comonomer content in the PHBV tested herein, which induces lower crystallinity and, hence, higher diffusivity to the vapor and gas molecules [18,51]. In the case of the commercial PET multilayer film, the permeance value was  $2.32 \times 10^{-11} \text{ kg}/\text{m}^2 \cdot \text{Pa} \cdot \text{s}$ , which corresponds to a permeability of  $2.25 \times 10^{-15} \text{ kg} \cdot \text{m}/\text{m}^2 \cdot \text{Pa} \cdot \text{s}$ , considering it as a monolayer material. The resultant WVTR was approximately  $6.3 \text{ g}/\text{m}^2 \cdot \text{day}$ , which is in the range but lower than the one reported by the manufacturer at  $38^\circ\text{C}$  and 90% RH, that is,  $16 \text{ g}/\text{m}^2 \cdot \text{day}$  [52] due to the lower temperature and humidity employed herein. Moreover, this water vapor permeability value is slightly lower than that of PET, that is,  $2.3 \times 10^{-15} \text{ kg} \cdot \text{m}/\text{m}^2 \cdot \text{Pa} \cdot \text{s}$ , measured at  $38^\circ\text{C}$  and 90% RH [53]. This can be related to the presence of a layer of polyolefin, such as LDPE, with a lower permeability, that is,  $1.2 \times 10^{-15} \text{ kg} \cdot \text{m}/\text{m}^2 \cdot \text{Pa} \cdot \text{s}$ , at  $38^\circ\text{C}$  and 90% RH [54]. This polyolefin layer is generally placed in the external part of the film in order to perform heat sealing at lower temperatures. In a food packaging context, both materials presented water vapor permeability between that of polyamide 6 (PA6), that is,  $2.06 \times 10^{-14} \text{ kg} \cdot \text{m}/\text{m}^2 \cdot \text{Pa} \cdot \text{s}$ , and PP, that is,  $7.26 \times 10^{-16} \text{ kg} \cdot \text{m}/\text{m}^2 \cdot \text{Pa} \cdot \text{s}$  [54]. One can further observe that the water permeance of the resultant PHBV/paper/PHBV multilayer was in the range of the PHBV film, but still significantly lower ( $p < 0.05$ ), with a value of  $4.48 \times 10^{-10} \text{ kg}/\text{m}^2 \cdot \text{Pa} \cdot \text{s}$ . This enhancement in the permeance can be mainly related to the increase in the thickness sample. However, it can also be ascribed to the fact that the hydrophobic PHBV film successfully protected paper from moisture and, thus, the barrier of paper improved in dry conditions. Similarly, the PET/paper/PET multilayer resulted in a value of  $1.91 \times 10^{-11} \text{ kg}/\text{m}^2 \cdot \text{Pa} \cdot \text{s}$  due to the higher water barrier performance and thickness of the petrochemical film.

As for the permeability of limonene, which is used as a standard to determine the aroma barrier, the paper presented a permeance of  $2.23 \times 10^{-9} \text{ kg}/\text{m}^2 \cdot \text{Pa} \cdot \text{s}$ , correspond-



ing to a permeability value of  $6.50 \times 10^{-13}$  kg·m/m<sup>2</sup>·Pa·s. Permeance of the PHBV film was  $5.80 \times 10^{-10}$  kg/m<sup>2</sup>·Pa·s, resulting in a permeability to limonene vapor of  $6.95 \times 10^{-15}$  kg·m/m<sup>2</sup>·Pa·s. This result indicates that the microbial copolyester was also much less permeable to aroma than paper. This result is relevant since limonene is known to be a good plasticizer for polyesters, such as PHAs and PET, and thus solubility plays a stronger role than diffusion in permeability. For example, it has been previously described that PHBV films of about 100 µm were able to adsorb 12.7 wt.% of limonene [49]. One can also observe that the permeance to limonene vapor of the PET-based multilayer film, the so-called PET film, was  $4.91 \times 10^{-11}$  kg/m<sup>2</sup>·Pa·s. This value is equivalent to a permeability of  $4.97 \times 10^{-15}$  kg·m/m<sup>2</sup>·Pa·s, assuming a monolayer material. Limonene permeability values for 75-µm PHB and PET films of 6.38 and  $6.43 \times 10^{-15}$  kg·m/m<sup>2</sup>·Pa·s have been respectively reported [55], which are relatively similar to the reported herein. In relation to the multilayers, the permeance values of PHBV/paper/PHB and PET/paper/PET multilayers were  $4.44 \times 10^{-10}$  and  $7.82 \times 10^{-11}$  kg/m<sup>2</sup>·Pa·s, respectively. Therefore, as it did with water vapor, the use of double coatings improved the aroma barrier of paper significantly ( $p < 0.05$ ). Although the improvement achieved with the PET film was significantly higher ( $p < 0.05$ ), one should consider that both polyesters resulted in a permeance reduction of nearly two orders of magnitude compared with uncoated paper, and the PHBV film thickness was lower.

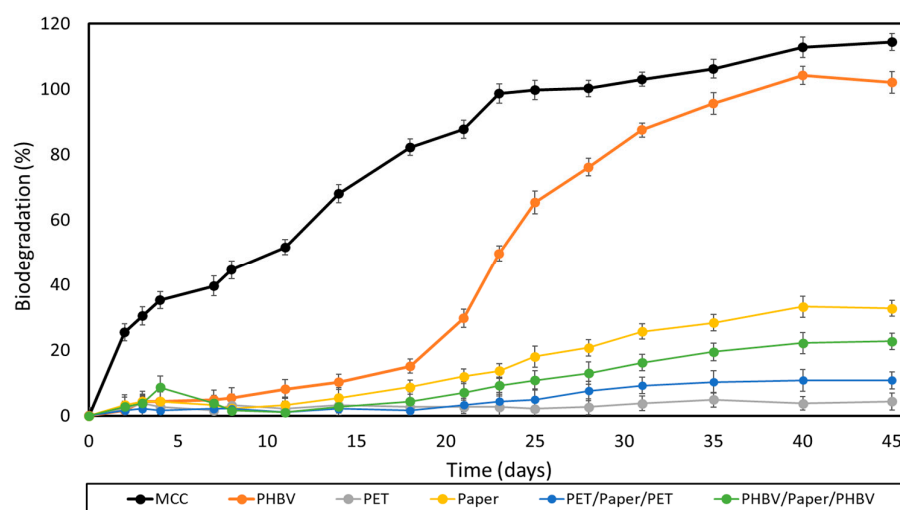
Regarding the oxygen barrier capacity, it was not possible to determine the oxygen permeance of the uncoated paper since it was above the detection limit (D.L.) of the equipment (OTR of 432.000 cm<sup>3</sup>/m<sup>2</sup>·day). The PHBV film presented a permeance to oxygen of  $2.41 \times 10^{-14}$  m<sup>3</sup>/m<sup>2</sup>·Pa·s. The oxygen permeance was previously determined for a 50-µm film of the same PHBV grade, resulting in a value of  $5.78 \times 10^{-15}$  m<sup>3</sup>/m<sup>2</sup>·Pa·s [56]. This permeance corresponds to an oxygen permeability of  $2.9 \times 10^{-19}$  m<sup>3</sup>·m/m<sup>2</sup>·Pa·s, which is nearly 50% higher than that of PHBV with 2–3 mol% 3HV; that is,  $2.1 \times 10^{-19}$  m<sup>3</sup>·m/m<sup>2</sup>·Pa·s [57]. The permeance to oxygen of the PET film was  $8.10 \times 10^{-16}$  m<sup>3</sup>/m<sup>2</sup>·Pa·s. This corresponds to a permeability of  $8.60 \times 10^{-20}$  m<sup>3</sup>·m/m<sup>2</sup>·Pa·s and an OTR of approximately 7.2 cm<sup>3</sup>/m<sup>2</sup>·day at 1 atm, assuming a monolayer material. Similar to WVTR, this value was also lower than the OTR values reported by the manufacturer, namely 14 and 20 cm<sup>3</sup>/m<sup>2</sup>·day when measured at 0 and 90% RH, respectively, at 1 bar and 23°C (ASTM D3985). This is related to the fact that EVOH and some condensation and relatively hydrophilic polymers, such as PET, present the highest barrier performance at low-to-intermediate moisture conditions (e.g., 20–60 %RH) [50]. At high humidity, the permeability to oxygen gas increases due to an increase in free volume by an effect of water-induced plasticization. At low humidity, the amount of sorbed water is not high enough to reach equilibrium for interchain hydrogen bonding so that the diffusion of the water molecules increases. One can finally observe that both multilayer sheets showed good oxygen-barrier performance, showing values of  $3.43 \times 10^{-15}$  and  $1.42 \times 10^{-16}$  m<sup>3</sup>/m<sup>2</sup>·Pa·s for the PHBV/paper/PHBV and PET/paper/PET samples, respectively. Interestingly, this represents a respective reduction of approximately 7 and 6 times when compared to the permeance of their respective single monolayer films used for the coatings. This permeance decrease can be ascribed to the use of double layers in the structure as well as the improved barrier performance to oxygen achieved in the paper at dry conditions when it was protected by the hydrophobic external layers. Therefore, the oxygen permeance of the paper sheets was successfully reduced by the application of the double coatings of biopolyester.

### 3.7. Compostability of Paper Multilayers

According to ISO 17088 [58], composting is the aerobic treatment of the biodegradable plastic parts of packaging waste that consumes oxygen and produces, under controlled conditions and using microorganisms, biomass, inorganic compounds, CO<sub>2</sub>, and water, without leaving visible distinguishable or toxic residues. Therefore, the evaluation of compostability includes three main tests, namely disintegration, biodegradation, and ecotoxicity [54,59,60]. Although recycling should be more economically and energetically

favorable than composting for paper packaging, it cannot be practical in some situations because of excessive sorting and cleaning requirements [61]. Therefore, compostability of paper multilayers can be relevant from a sustainable point of view of waste management. This is particularly relevant when recycling is not feasible, for instance, in the case of disposable containers contaminated with food residues.

The ripe compost used as inoculum in both the biodegradation and disintegration tests showed an initial organic matter content (VS) of  $90\% \pm 0.9\%$ , expressed as volatile solids with respect to dried solids. The content of total dry solids (DS) was  $79\% \pm 1.3\%$ , whereas the pH value was 8.1, measured according to ISO 14855. Figure 7 shows the results of the aerobic biodegradation test of the films and paper sheets under controlled composting conditions ( $58 \pm 2^\circ\text{C}$  for 45 days) following the method adapted from the ISO 14855. This test is based on the measurement of the  $\text{CO}_2$  generated in the biodegradation process, which is considered proportional to the percentage of biodegradation in organic samples. MCC was also tested and used as positive reference. Moreover, the theoretical maximum quantity of  $\text{CO}_2$  that can be produced by the biodegradation of the samples was calculated from their theoretical carbon content.

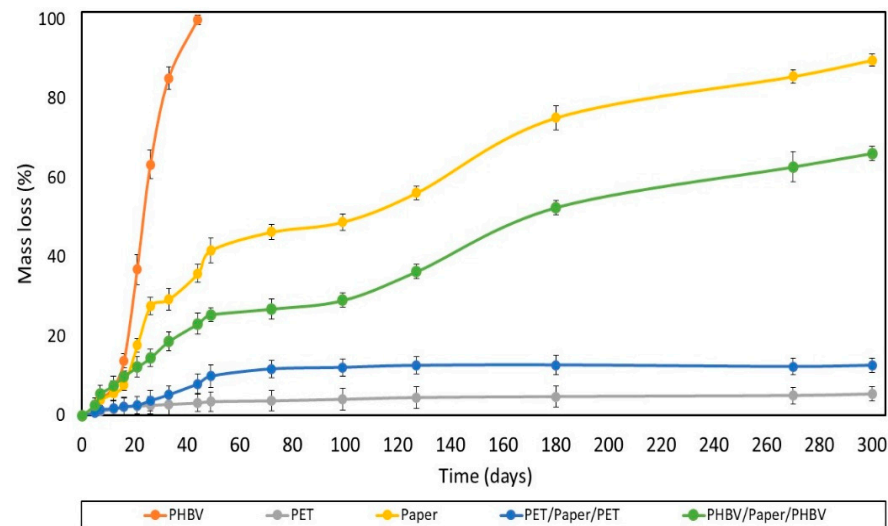


**Figure 7.** Sample biodegradation as a function of time of microcrystalline cellulose (MCC), the paper sheet, poly(3-hydroxybutyrate-co-3-hydroxyvalerate) (PHBV) and polyethylene terephthalate (PET) films, and PHBV/paper/PHBV and PET/paper/PET multilayer sheets.

One can observe that both MCC and the PHBV film completely biodegraded after 28 days and 40 days, respectively. Moreover, these samples exhibited the characteristic sigmoid profiles of respirometric tests, showing three different phases [60,62]. In the case of the PHBV film, it presented an initial lag period of 2–15 days, followed by a biodegradation phase that was prolonged up to day 40, and finished with a plateau. PHBV biodegradation is essentially an enzymatic process, where exoenzymes from bacteria and fungi or membrane-bound enzymes, such as proteases, lipases, and esterases, which are present in the composting soil, hydrolyze the biopolymer chains into their corresponding monomers (hydroxy acids) [63]. In this process, the microorganisms first colonize the surface of the biopolymer and then secrete depolymerases that hydrolyze the ester bonds. This process yields to low- $M_w$  chains able to pass through the semipermeable external bacterial membranes and are metabolized. MCC, after 45 days, reached a biodegradation percentage of  $\sim 115\%$ , which is attributed to the “priming” effect. The latter is an overestimation of the  $\text{CO}_2$  released that occurs when the compost inoculum in the test reactor containing the samples generates more  $\text{CO}_2$  than the compost inoculum in the blank reactors [64]. This effect has been previously ascribed to the stimulation of organic matter mineralization that takes place after the addition of easily-decomposable organic matter [65]. As expected, the commercial multilayer film showed no biodegradation since this is based on polymers that

are not biodegradable. The uncoated paper reached a value of nearly 33%, whereas the PHBV- and PET-double coated papers showed lower biodegradation values, of 23 and 11%, respectively. In all cases, the so-called plateau phase was reached, showing a minor upward slope still noticeable in the curves. This means that biodegradation could continue under the same conditions by degrading the remaining organic carbon. However, since none of the paper samples exceeded the 70% biodegradation limit after 45 days, these cannot be considered as compostable under the conditions established by the standard. This was particularly notable for the PET/paper/PET multilayer due to the non-biodegradability of the petrochemical films. Therefore, it is advisable to avoid its incorporation into compostability plants. These results agree with those of the study performed by López Alvarez et al. [66], who showed that papers do not achieve the same level of biodegradation as MCC after 45 days. This is due to other organic compounds present in commercial paper, for example, lignocellulose and fatty acids, which can retard biodegradation. Furthermore, the large thickness of the paper sheets has to be also considered, 290  $\mu\text{m}$ , which can highly reduce the biodegradation rate of biodegradable materials [67].

The degree of disintegration after 300 days ( $\%D_{300}$ ) of the films and sheets exposed to laboratory-scale composting environmental conditions ( $58 \pm 2^\circ\text{C}$ ) was also analyzed, providing information about the physical breakdown of the samples into smaller fractions with time. The test was validated according to the standard method [31], which establishes a reduction (R) of the volatile-solid content in the sample of the compost of more than 30%, with a standard deviation for  $\%D_{300}$  values of less than 10 units. In the performance tests, R for the uncoated paper sheet was  $57 \pm 2$ , and the standard deviations for  $\%D_{300}$  values were lower than 10. Figure 8 shows the disintegration values (% mass loss) as a function of time of the different films and sheets. As can be observed, the neat PHBV film fully disintegrated after 44 days, in agreement with previous works [68]. The disintegration rate was low during the first 12 days, then mass loss occurred very fast, and finally the rate slowed down after 40 days. In contrast, the commercial PET-based multilayer film showed mass loss values below 1%, which can be mainly related to losses occurring during the experimental preparation and manipulation of the samples.

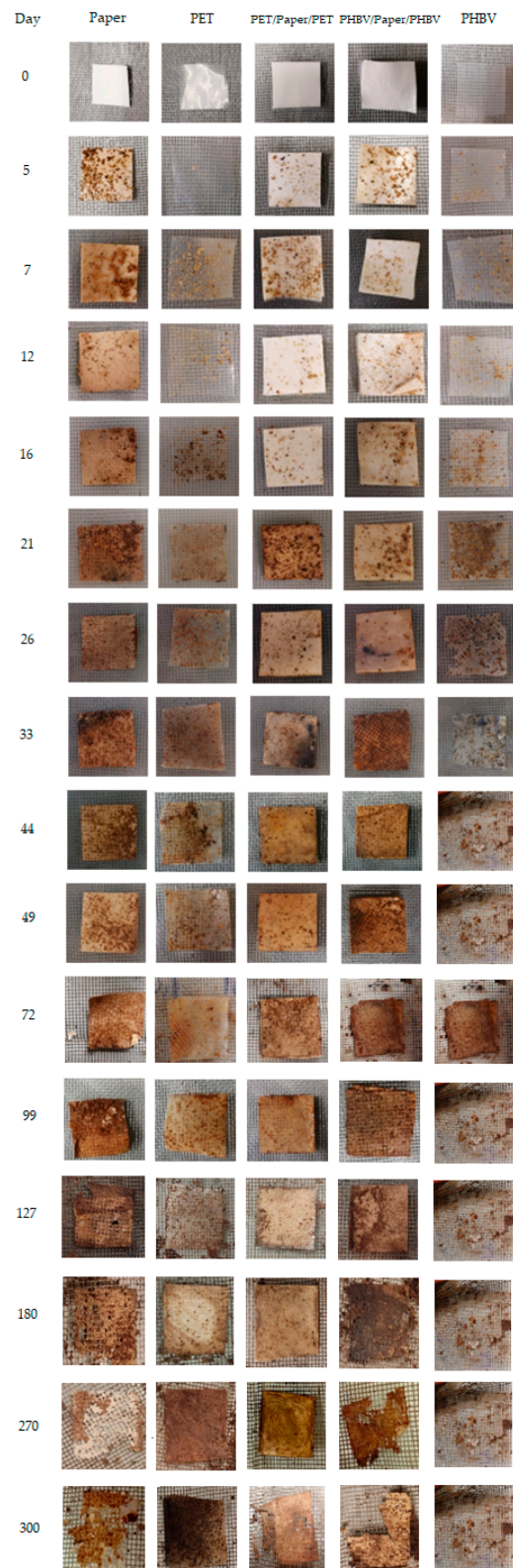


**Figure 8.** Disintegration rate under composting conditions of the paper sheet, poly(3-hydroxybutyrate-co-3-hydroxyvalerate) (PHBV) and polyethylene terephthalate (PET) films, and PHBV/paper/PHBV and PET/paper/PET multilayer sheets.

One can observe that all the paper sheets showed similar disintegration patterns. These presented three stages, clearly distinguished in the tested composting conditions, as similarly reported by Seoane et al. [69]. In the first step, corresponding to the period of 2–15 days, a low degree of disintegration was observed. In the second one, the dis-

integration rate markedly increased throughout 50 days till reaching a plateau. In this stage, the greatest disintegration rate was observed for the uncoated paper, confirming that the film coatings delayed the composting of paper. This delay can be related to the lower water absorption attained in the coated paper sheets due to the hydrophobic character of the polymers. Thus, the films impaired hydrolysis of paper into smaller molecules and the enzymatic reactions associated with the microbial growth as well as the ingress and colonization of microorganisms. Moreover, the higher compaction and lower porosity of the paper present in the multilayer (as consequence of the thermo-sealing process) could also contribute to the higher resistance to enzymatic degradation of the coated paper. This delay was significantly ( $p < 0.05$ ) higher in the PET/paper/PET sheet due to the lack of biodegradability of the petrochemical polymers. Moreover, the multilayer structures are prone to present a considerably high amount of biodegradation products accumulated on the sheet-film interphases, which could retard degradation due to diffusional limitations [70]. After 300 days, all the paper sheets maintained practically the same rate of degradation, reaching %D<sub>300</sub> values of approximately 90%, 70%, and 15% for the uncoated and PHBV- and PET-double-coated paper sheets, respectively. The difference attained between the PHBV/paper/PHBV and PET/paper/PET multilayer sheets can mainly be attributed to the disintegration of the PHBV thin film in the compost. Indeed, PET-double-coated paper exhibited intermediate disintegration behavior between those observed for its counterpart monolayer materials, that is, the paper sheet and PET film, but it was closer to that of the petrochemical film. This can be related to the partial and slow degradation of the inner paper layer, which was only available for microbial attack through the edges of the multilayer sample. In contrast, the biodegradation pattern of the paper sheet double coated with PHBV was similar to that of the uncoated paper sheet, although the disintegration was lower than that expected considering the mass loss observed in the monolayers. In particular, from the linear trend observed during the last disintegration stage of the uncoated and PHBV/paper/PHBV sheet samples, it was estimated that approximately 350 and 475 days would be required, respectively, to reach a 100% reduction of the original mass. In any case, none of the paper-based sheets tested herein were compostable since, after 3 months, their mass did not amount to less than 10% of their original mass.

Finally, Figure 9 illustrates the visual appearance of the recovered films and sheets after the selected times of disintegration, where the different degradable characters of the samples can be observed. At the beginning of the process, all of the film and sheet samples exhibited a continuous structure with no visible holes, but they showed an increase in opacity during the first week. At the third week, signs of erosion were detected in some of the samples. Then, the PHBV film fully disintegrated after 44 days, whereas the PET film developed a brown color without signs of mass loss but with high amounts of compost particles adhered on the surface. All the paper sheets showed certain signs of erosion and small fractures after 100 days of incubation in the compost. One can further observe that after 180 days, the uncoated paper and PHBV/paper/PHBV sheets appeared broken into small parts, particularly the uncoated sample, whereas the PET/paper/PET sheet still maintained its full integrity. Finally, after 300 days, the uncoated paper was hardly distinguishable from compost in the mesh due to the fact that the aggregates were brown. In the case of PHBV/paper/PHBV, some fragments smaller than the mesh size were formed.



**Figure 9.** Photographs taken at different composting times of the paper sheet, poly(3-hydroxybutyrate-co-3-hydroxyvalerate) (PHBV) and polyethylene terephthalate (PET) films, and PHBV/paper/PHBV and PET/paper/PET multilayer sheets.

#### 4. Conclusions

PHBV has been proven to be an excellent material for paper coating applications. By means of heat-sealing technology, which is currently available in the food packaging industry, for instance in lamination or thermoforming processes, PHBV/paper/PHBV multilayers with improved mechanical and barrier properties were successfully obtained. Moreover, the presence of the double coatings of PHBV did not notably affect the original optical and thermal characteristics of the paper. Although the performance was lower than that of equivalent multilayers developed by the same process using conventional PET-based films with high barrier, the properties presented here by the double-coated biopolymer structures were within the same range. Thus, it can be concluded that PHBV/paper/PHBV multilayer sheets can be excellent candidates to replace currently available paper substrates coated with petrochemical non-biodegradable films, especially in the case of rigid and intermediate barrier packaging materials. However, to meet current requirements to be certified as compostable, paper layers with lower thickness would be required. Future works will focus on developing novel biopolymer/paper trays and their application in packaging, particularly for the preservation of foodstuffs with high water activity, where the use of paper is restricted. Additionally, their food safety assessment will be ascertained by migration tests using food simulants.

**Author Contributions:** Conceptualization, P.Z. and S.T.-G.; methodology, E.H.-G. and P.A.V.F.; formal analysis, E.H.-G. and P.A.V.F.; investigation, E.H.-G. and P.A.V.F.; data curation, E.H.-G. and P.A.V.F.; writing—original draft preparation, E.H.-G.; writing—review and editing, C.G.-M. and S.T.-G.; supervision, C.G.-M. and S.T.-G.; project administration, S.T.-G.; funding acquisition, P.Z. and S.T.-G. All authors have read and agreed to the published version of the manuscript.

**Funding:** This research was funded by the Spanish Ministry of Science and Innovation (MICI), grant number PID2021-128749OB-C33 and the Valencian Innovation Agency (AVI) through the TERMOFIB project (INNVA1/2020/46).

**Institutional Review Board Statement:** Not applicable.

**Informed Consent Statement:** Not applicable.

**Data Availability Statement:** Data are contained within the article and also available on request.

**Acknowledgments:** E.H.-G. and S.T.-G. acknowledge MICI for her predoctoral research grant (BES 2017-082040) and Ramón y Cajal for his contract (RYC2019-027784-I), respectively.

**Conflicts of Interest:** The authors declare no conflict of interest.

#### References

1. Torres-Giner, S.; Gil, L.; Pascual-Ramírez, L.; Garde-Belza, J.A. Packaging: Food Waste Reduction. In *Encyclopedia of Polymer Applications*; CRC Press: Boca Raton, FL, USA, 2019. [\[CrossRef\]](#)
2. Lagarón, J.M.; Cabedo, L.; Cava, D.; Feijoo, J.L.; Gavara, R.; Gimenez, E. Improving packaged food quality and safety. Part 2: Nanocomposites. *Food Addit. Contam.* **2005**, *22*, 994–998. [\[CrossRef\]](#) [\[PubMed\]](#)
3. Torres-Giner, S.; Figueroa-Lopez, K.J.; Melendez-Rodriguez, B.; Prieto, C.; Pardo-Figuerez, M.; Lagaron, J.M. Emerging Trends in Biopolymers for Food Packaging. In *Sustainable Food Packaging Technology*; John Wiley & Sons, Ltd.: Hoboken, NJ, USA, 2021; pp. 1–33. [\[CrossRef\]](#)
4. Hale, R.C.; Seeley, M.E.; La Guardia, M.J.; Mai, L.; Zeng, E.Y. A Global Perspective on Microplastics. *J. Geophys. Res. Ocean.* **2020**, *125*, e2018JC014719. [\[CrossRef\]](#)
5. Cverenkárová, K.; Valachovičová, M.; Mackul'ak, T.; Žemlička, L.; Bírošová, L. Microplastics in the Food Chain. *Life* **2021**, *11*, 1349. [\[CrossRef\]](#) [\[PubMed\]](#)
6. Nakaya, M.; Uedono, A.; Hotta, A. Recent Progress in Gas Barrier Thin Film Coatings on PET Bottles in Food and Beverage Applications. *Coatings* **2015**, *5*, 987–1001. [\[CrossRef\]](#)
7. Alias, A.R.; Wan, M.K.; Sarbon, N.M. Emerging materials and technologies of multi-layer film for food packaging application: A review. *Food Control* **2022**, *136*, 108875. [\[CrossRef\]](#)
8. Zhong, Y.; Godwin, P.; Jin, Y.; Xiao, H. Biodegradable polymers and green-based antimicrobial packaging materials: A mini-review. *Adv. Ind. Eng. Polym. Res.* **2020**, *3*, 27–35. [\[CrossRef\]](#)

9. Gabirondo, E.; Melendez-Rodriguez, B.; Arnal, C.; Lagaron, J.M.; Martínez De Ilarduya, A.; Sardon, H.; Torres-Giner, S. Organocatalyzed closed-loop chemical recycling of thermo-compressed films of poly(ethylene furanoate). *Polym. Chem.* **2021**, *12*, 1571–1580. [[CrossRef](#)]
10. Guillard, V.; Gaucel, S.; Fornaciari, C.; Angellier-Coussy, H.; Buche, P.; Gontard, N. The Next Generation of Sustainable Food Packaging to Preserve Our Environment in a Circular Economy Context. *Front. Nutr.* **2018**, *5*, 121. [[CrossRef](#)]
11. Pojanavaraphan, T.; Magaraphan, R.; Chiou, B.-S.; Schiraldi, D.A. Development of Biodegradable Foamlike Materials Based on Casein and Sodium Montmorillonite Clay. *Biomacromolecules* **2010**, *11*, 2640–2646. [[CrossRef](#)]
12. Vartiainen, J.; Shen, Y.; Kaljunen, T.; Malm, T.; Vähä-Nissi, M.; Putkonen, M.; Harlin, A. Bio-based multilayer barrier films by extrusion, dispersion coating and atomic layer deposition. *J. Appl. Polym. Sci.* **2016**, *133*. [[CrossRef](#)]
13. Arcos-Hernández, M.V.; Laycock, B.; Donose, B.C.; Pratt, S.; Halley, P.; Al-Luaibi, S.; Werker, A.; Lant, P.A. Physicochemical and mechanical properties of mixed culture polyhydroxyalkanoate (PHBV). *Eur. Polym. J.* **2013**, *49*, 904–913. [[CrossRef](#)]
14. Bucci, D.Z.; Tavares, L.B.B.; Sell, I. Biodegradation and physical evaluation of PHB packaging. *Polym. Test.* **2007**, *26*, 908–915. [[CrossRef](#)]
15. Kamravamanesh, D.; Kovacs, T.; Pflügl, S.; Druzhinina, I.; Kroll, P.; Lackner, M.; Herwig, C. Increased poly- $\beta$ -hydroxybutyrate production from carbon dioxide in randomly mutated cells of cyanobacterial strain *Synechocystis* sp. PCC 6714: Mutant generation and characterization. *Bioresour. Technol.* **2018**, *266*, 34–44. [[CrossRef](#)]
16. Peelman, N.; Ragaert, P.; De Meulenaer, B.; Adons, D.; Peeters, R.; Cardon, L.; Van Impe, F.; Devlieghere, F. Application of bioplastics for food packaging. *Trends Food Sci. Technol.* **2013**, *32*, 128–141. [[CrossRef](#)]
17. Fabra, M.J.; Sánchez, G.; López-Rubio, A.; Lagaron, J.M. Microbiological and ageing performance of polyhydroxyalkanoate-based multilayer structures of interest in food packaging. *LWT-Food Sci. Technol.* **2014**, *59*, 760–767. [[CrossRef](#)]
18. Modi, S.; Koelling, K.; Vodovotz, Y. Assessment of PHB with varying hydroxyvalerate content for potential packaging applications. *Eur. Polym. J.* **2011**, *47*, 179–186. [[CrossRef](#)]
19. Keshavarz, T.; Roy, I. Polyhydroxyalkanoates: Bioplastics with a green agenda. *Curr. Opin. Microbiol.* **2010**, *13*, 321–326. [[CrossRef](#)]
20. Laycock, B.; Arcos-Hernandez, M.V.; Langford, A.; Pratt, S.; Werker, A.; Halley, P.J.; Lant, P.A. Crystallisation and fractionation of selected polyhydroxyalkanoates produced from mixed cultures. *New Biotechnol.* **2014**, *31*, 345–356. [[CrossRef](#)]
21. Laycock, B.; Halley, P.; Pratt, S.; Werker, A.; Lant, P. The chemomechanical properties of microbial polyhydroxyalkanoates. *Prog. Polym. Sci.* **2013**, *38*, 536–583. [[CrossRef](#)]
22. Anderson, A.J.; Dawes, E.A. Occurrence, metabolism, metabolic role, and industrial uses of bacterial polyhydroxyalkanoates. *Microbiol. Rev.* **1990**, *54*, 450–472. [[CrossRef](#)]
23. Ebnesajjad, S. *Handbook of Biopolymers and Biodegradable Plastics: Properties, Processing and Applications*; Elsevier: Amsterdam, The Netherlands, 2013; pp. 1–462. [[CrossRef](#)]
24. Savenkova, L.; Gerberga, Z.; Bibers, I.; Kalnin, M. Effect of 3-hydroxy valerate content on some physical and mechanical properties of polyhydroxyalkanoates produced by *Azotobacter chroococcum*. *Process. Biochem.* **2000**, *36*, 445–450. [[CrossRef](#)]
25. Hutchings, J.B. Food and Colour Appearance. In *Chapman and Hall Food Science Book*, 2nd ed.; Aspen Publication: Gaithersburg, MD, USA, 1999.
26. Agüero, A.; Morcillo, M.D.C.; Quiles-Carrillo, L.; Balart, R.; Boronat, T.; Lascano, D.; Torres-Giner, S.; Fenollar, O. Study of the Influence of the Reprocessing Cycles on the Final Properties of Polylactide Pieces Obtained by Injection Molding. *Polymers* **2019**, *11*, 1908. [[CrossRef](#)] [[PubMed](#)]
27. ASTM D882; Standard Test Method for Tensile Properties of Thin Plastic Sheeting. American Society for Testing and Materials: Philadelphia, PA, USA, 2001; pp. 162–170.
28. ASTM E96/E96M; Standard Test Methods for Water Vapor Transmission of Materials. American Society for Testing and Materials: Philadelphia, PA, USA, 2005; pp. 406–413.
29. ASTM 3985-95; Standard Test Method for Oxygen Gas Transmission Rate through Plastic Film and Sheeting Using a Coulometric Sensor. American Society for Testing and Materials: Philadelphia, PA, USA, 2002; pp. 472–477.
30. UNE-EN ISO 14855-1; Asociación Española de Normalización. Determinación de la Biodegradabilidad Aeróbica Final de Materiales Plásticos en Condiciones de Compostaje Controladas. Método Según el Análisis de Dióxido de Carbono Generado. Parte 1; Método General. Asociación Española de Normalización: Madrid, Spain, 2012.
31. ISO 20200. Plastics-Determination of the Degree of Disintegration of Plastic Materials under Simulated Composting in a Laboratory -Scale Test. 2004. Available online: <https://www.une.org> (accessed on 15 November 2022).
32. Melendez-Rodriguez, B.; Reis, M.A.M.; Carvalheira, M.; Sammon, C.; Cabedo, L.; Torres-Giner, S.; Lagaron, J.M. Development and Characterization of Electrospun Biopapers of Poly(3-hydroxybutyrate-co-3-hydroxyvalerate) Derived from Cheese Whey with Varying 3-Hydroxyvalerate Contents. *Biomacromolecules* **2021**, *22*, 2935–2953. [[CrossRef](#)] [[PubMed](#)]
33. Cherpinski, A.; Torres-Giner, S.; Cabedo, L.; Méndez, J.A.; Lagaron, J.M. Multilayer structures based on annealed electrospun biopolymer coatings of interest in water and aroma barrier fiber-based food packaging applications. *J. Appl. Polym. Sci.* **2018**, *135*, 45501. [[CrossRef](#)]
34. Ivorra-Martinez, J.; Quiles-Carrillo, L.; Boronat, T.; Torres-Giner, S.; A Covas, J. Assessment of the Mechanical and Thermal Properties of Injection-Molded Poly(3-hydroxybutyrate-co-3-hydroxyhexanoate)/Hydroxyapatite Nanoparticles Parts for Use in Bone Tissue Engineering. *Polymers* **2020**, *12*, 1389. [[CrossRef](#)]
35. Hernández-García, E.; Vargas, M.; Torres-Giner, S. Quality and Shelf-Life Stability of Pork Meat Fillets Packaged in Multilayer Polylactide Films. *Foods* **2022**, *11*, 426. [[CrossRef](#)]

36. Ortega-Toro, R.; Jiménez, A.; Talens, P.; Chiralt, A. Properties of starch–hydroxypropyl methylcellulose based films obtained by compression molding. *Carbohydr. Polym.* **2014**, *109*, 155–165. [CrossRef]
37. Villalobos, R.; Chanona, J.; Hernández, P.; Gutiérrez, G.; Chiralt, A. Gloss and transparency of hydroxypropyl methylcellulose films containing surfactants as affected by their microstructure. *Food Hydrocoll.* **2005**, *19*, 53–61. [CrossRef]
38. Torres-Giner, S.; Hilliou, L.; Melendez-Rodríguez, B.; Figueroa-Lopez, K.J.; Madalena, D.; Cabedo, L.; Covas, J.A.; Vicente, A.A.; Lagaron, J.M. Melt processability, characterization, and antibacterial activity of compression-molded green composite sheets made of poly(3-hydroxybutyrate-co-3-hydroxyvalerate) reinforced with coconut fibers impregnated with oregano essential oil. *Food Packag. Shelf Life* **2018**, *17*, 39–49. [CrossRef]
39. Lennersten, M.; Lingnert, H. Influence of Wavelength and Packaging Material on Lipid Oxidation and Colour Changes in Low-fat Mayonnaise. *LWT Food Sci. Technol.* **2000**, *33*, 253–260. [CrossRef]
40. Costa, M.; Pastrana, L.M.; Teixeira, J.A.; Sillankorva, S.M.; Cerqueira, M. Characterization of PHBV films loaded with FO1 bacteriophage using polyvinyl alcohol-based nanofibers and coatings: A comparative study. *Innov. Food Sci. Emerg. Technol.* **2021**, *69*, 102646. [CrossRef]
41. Velásquez, E.; Garrido, L.; Valenzuela, X.; Galotto, M.J.; Guarda, A.; López de Dicastillo, C. Physical properties and safety of 100% post-consumer PET bottle -organoclay nanocomposites towards a circular economy. *Sustain. Chem. Pharm.* **2020**, *17*, 100285. [CrossRef]
42. Mahy, M.; Eycken, L.; Oosterlinck, A. Evaluation of Uniform Color Spaces Developed after the adoption of CIELAB and CIELUV. *Color Res. Appl.* **1994**, *19*, 105–121.
43. Melendez-Rodríguez, B.; Torres-Giner, S.; Aldureid, A.; Cabedo, L.; Lagaron, J.M. Reactive Melt Mixing of Poly(3-Hydroxybutyrate)/Rice Husk Flour Composites with Purified Biosustainably Produced Poly(3-Hydroxybutyrate-co-3-Hydroxyvalerate). *Materials* **2019**, *12*, 2152. [CrossRef]
44. Yang, H.; Yan, R.; Chen, H.; Lee, D.H.; Zheng, C. Characteristics of hemicellulose, cellulose and lignin pyrolysis. *Fuel* **2007**, *86*, 1781–1788. [CrossRef]
45. Souza, B.S.; Moreira, A.P.D.; Teixeira, A.M.R.F. TG-FTIR coupling to monitor the pyrolysis products from agricultural residues. *J. Therm. Anal. Calorim.* **2009**, *97*, 637. [CrossRef]
46. Bugnicourt, E.; Cinelli, P.; Lazzeri, A.; Álvarez, V.A. Polyhydroxyalkanoate (PHA): Review of synthesis, characteristics, processing and potential applications in packaging. *Express Polym. Lett.* **2014**, *8*, 791–808. [CrossRef]
47. Levchik, S.V.; Weil, E.D. A review on thermal decomposition and combustion of thermoplastic polyesters. *Polym. Adv. Technol.* **2004**, *15*, 691–700. [CrossRef]
48. Deshwal, G.K.; Panjagari, N.R.; Alam, T. An overview of paper and paper-based food packaging materials: Health safety and environmental concerns. *J. Food Sci. Technol.* **2019**, *56*, 4391–4403. [CrossRef]
49. Sanchez-Garcia, M.D.; Gimenez, E.; Lagaron, J.M. Morphology and barrier properties of solvent cast composites of thermoplastic biopolymers and purified cellulose fibers. *Carbohydr. Polym.* **2008**, *71*, 235–244. [CrossRef]
50. Melendez-Rodríguez, B.; Torres-Giner, S.; Angulo, I.; Pardo-Figueroa, M.; Hilliou, L.; Escuin, J.M.; Cabedo, L.; Nevo, Y.; Prieto, C.; Lagaron, J.M. High-Oxygen-Barrier Multilayer Films Based on Polyhydroxyalkanoates and Cellulose Nanocrystals. *Nanomaterials* **2021**, *11*, 1443. [CrossRef] [PubMed]
51. Nduko, J.M.; Matsumoto, K.; Taguchi, S. Biological lactate-polymers synthesized by one-pot microbial factory: Enzyme and metabolic engineering. *ACS Symp. Ser.* **2012**, *1105*, 213–235.
52. ASTM F1249; Standard Test Method for Water Vapor Transmission Rate through Plastic Film and Shetting Using a Modulated Infrared Sensor. American Society for Testing and Materials: Philadelphia, PA, USA, 2020.
53. Lagarón, J.M. 1-Multifunctional and nanoreinforced polymers for food packaging. In *Multifunctional and Nanoreinforced Polymers for Food Packaging*; Lagarón, J.-M., Ed.; Woodhead Publishing: Sawston, UK, 2011.
54. Balaguer, M.P.; Villanova, J.; Cesar, G.; Gavara, R.; Hernandez-Munoz, P. Compostable properties of antimicrobial bioplastics based on cinnamaldehyde cross-linked gliadins. *Chem. Eng. J.* **2015**, *262*, 447–455. [CrossRef]
55. Fabra, M.J.; Lopez-Rubio, A.; Lagaron, J.M. Nanostructured interlayers of zein to improve the barrier properties of high barrier polyhydroxyalkanoates and other polyesters. *J. Food Eng.* **2014**, *127*, 1–9. [CrossRef]
56. Melendez-Rodríguez, B.; Torres-Giner, S.; Zavagna, L.; Sammon, C.; Cabedo, L.; Prieto, C.; Lagaron, J.M. Development and Characterization of Electrospun Fiber-Based Poly(ethylene-co-vinyl Alcohol) Films of Application Interest as High-Gas-Barrier Interlayers in Food Packaging. *Polymers* **2021**, *13*, 2061. [CrossRef]
57. Quiles-Carrillo, L.; Montanes, N.; Lagaron, J.M.; Balart, R.; Torres-Giner, S. In Situ Compatibilization of Biopolymer Ternary Blends by Reactive Extrusion with Low-Functionality Epoxy-Based Styrene–Acrylic Oligomer. *J. Polym. Environ.* **2019**, *27*, 84–96. [CrossRef]
58. ISO 17088. Specifications for compostable plastics. 2012. Available online: <https://www.iso.org/obp/ui/#iso:std:iso:17088:ed-2:v1:en> (accessed on 4 November 2022).
59. Hernández-García, E.; Vargas, M.; González-Martínez, C.; Chiralt, A. Biodegradable Antimicrobial Films for Food Packaging: Effect of Antimicrobials on Degradation. *Foods* **2021**, *10*, 1256. [CrossRef]
60. Hernández-García, E.; Vargas, M.; Chiralt, A.; González-Martínez, C. Biodegradation of PLA-PHBV Blend Films as Affected by the Incorporation of Different Phenolic Acids. *Foods* **2022**, *11*, 243. [CrossRef]



61. Kale, G.; Kijchavengkul, T.; Auras, R.; Rubino, M.; Selke, S.E.; Singh, S.P. Compostability of Bioplastic Packaging Materials: An Overview. *Macromol. Biosci.* **2007**, *7*, 255–277. [[CrossRef](#)]
62. Cano, A.I.; Cháfer, M.; Chiralt, A.; González-Martínez, C. Biodegradation behavior of starch-PVA films as affected by the incorporation of different antimicrobials. *Polym. Degrad. Stab.* **2016**, *132*, 11–20. [[CrossRef](#)]
63. Iglesias-Montes, M.L.; Soccio, M.; Luzi, F.; Puglia, D.; Gazzano, M.; Lotti, N.; Manfredi, L.B.; Cyras, V.P. Evaluation of the Factors Affecting the Disintegration under a Composting Process of Poly(lactic acid)/Poly(3-hydroxybutyrate) (PLA/PHB) Blends. *Polymers* **2021**, *13*, 3171. [[CrossRef](#)]
64. Shen, J.; Bartha, R. Priming effect of glucose polymers in soil-based biodegradation tests. *Soil Biol. Biochem.* **1997**, *29*, 1195–1198. [[CrossRef](#)]
65. Kuzyakov, Y.; Friedel, J.K.; Stahr, K. Review of mechanisms and quantification of priming effects. *Soil Biol. Biochem.* **2000**, *32*, 1485–1498. [[CrossRef](#)]
66. López Alvarez, J.V.; Aguilar Larrucea, M.; Arraiza Bermúdez, P.; León Chicote, B. Biodegradation of paper waste under controlled composting conditions. *Waste Manag.* **2009**, *29*, 1514–1519. [[CrossRef](#)]
67. Rojas-Lema, S.; Arevalo, J.; Gomez-Caturra, J.; Garcia-Garcia, D.; Torres-Giner, S. Peroxide-Induced Synthesis of Maleic Anhydride-Grafted Poly(butylene succinate) and Its Compatibilizing Effect on Poly(butylene succinate)/Pistachio Shell Flour Composites. *Molecules* **2021**, *26*, 5927. [[CrossRef](#)]
68. Lidón Sánchez-Safont, E.; González-Ausejo, J.; Gámez-Pérez, J.; Lagarón, J.M.; Cabedo, L. Poly(3-Hydroxybutyrate-co-3-Hydroxyvalerate)/ Purified Cellulose Fiber Composites by Melt Blending: Characterization and Degradation in Composting Conditions. *J. Renew. Mater.* **2016**, *4*, 123. [[CrossRef](#)]
69. Seoane, I.T.; Luzi, F.; Puglia, D.; Cyras, V.P.; Manfredi, L.B. Enhancement of paperboard performance as packaging material by layering with plasticized polyhydroxybutyrate/nanocellulose coatings. *J. Appl. Polym. Sci.* **2018**, *135*, 46872. [[CrossRef](#)]
70. Bi, S.; Pan, H.; Barinelli, V.; Eriksen, B.; Ruiz, S.; Sobkowicz, M.J. Biodegradable polyester coated mulch paper for controlled release of fertilizer. *J. Clean. Prod.* **2021**, *294*, 126348. [[CrossRef](#)]

**Disclaimer/Publisher’s Note:** The statements, opinions and data contained in all publications are solely those of the individual author(s) and contributor(s) and not of MDPI and/or the editor(s). MDPI and/or the editor(s) disclaim responsibility for any injury to people or property resulting from any ideas, methods, instructions or products referred to in the content.